BOREAS An international journal of Quaternary research

Holocene evolution of a proglacial lake in southern Kamchatka, Russian Far East

LARISA NAZAROVA, DIRK SACHSE, HARALD G. E. FUCHS, VERONIKA DIRKSEN, OLEG DIRKSEN, LIUDMILA SYRYKH, NADEZHDA G. RAZJIGAEVA, OLIVER RACH AND BERNHARD DIEKMANN

BOREAS

Nazarova, L., Sachse, D., Fuchs, H. G. E., Dirksen, V., Dirksen, O., Syrykh, L., Razjigaeva,, N. G., Rach, O. & Diekmann B. 2021 (October): Holocene evolution of a proglacial lake in southern Kamchatka, Russian Far East. *Boreas*, Vol. 50, pp. 1011–1026. https://doi.org/10.1111/bor.12554. ISSN 0300-9483.

The Kamchatka Peninsula (Russian Far East) remains among the least studied regions of eastern Asia. Recent studies revealed a high degree of palaeoenvironmental variability between different parts of the peninsula. We investigated semi-aquatic (chironomids) and terrestrial (leaf wax biomarkers) proxies from a sediment core collected from Lake Sokoch (southern Kamchatka) to provide reconstruction of the mean July air temperature and variations in limnic conditions. The lake formed after 10.0 cal. ka BP as a result of postglacial warming and was fed by glacial meltwaters from neighbouring glaciers. Our data show a later beginning of the Holocene thermal maximum (HTM) relative to more northern sites in Kamchatka, Siberia and Chukotka and support climate model experiments that suggest that the HTM was delayed in southern and central Kamchatka by about 2000 years compared with Alaska and NE Siberia. Warm conditions prevailed between 10.0 and 6.4 cal. ka BP with a short spell of cool and dry climate around 8.2 cal. ka BP that might be related to the 8.2 ka cooling event. The HTM took place between 6.5 and 3.4 cal. ka BP with the warmest phase from 6.0 to 5.0 cal. ka BP. An onset of Neoglacial cooling at 3.4 cal. ka BP is consistent with the strengthening of both the Siberian High and the Aleutian Low. Warming between 1.2 and 0.9 cal. ka BP can be attributed to the Mediaeval Climate Anomaly. The LIA cooling is related to another strengthening of the Siberian High and the Aleutian Low. The modern warming, though weakly traced in our record, is consistent with the recent meteorological observations. The presented palaeoenvironment record confirms the earlier findings of spatial differences within Kamchatka in timing and magnitude of the major Holocene climate fluctuations and contributes towards understanding the expression of Holocene climate change in Kamchatka.

Larisa Nazarova (larisa.nazarova@awi.de) and Bernhard Diekmann, Alfred Wegener Institute Helmholtz Centre for Polar and Marine Research, Research Unit Potsdam, Telegrafenberg A43, 14473 Potsdam, Germany and University of Potsdam, Institute of Geosciences, Karl-Liebknecht-str. 24-25, 14476 Potsdam-Golm, Germany; Dirk Sachseand Oliver Rach, Helmholtz-Centre Potsdam-GFZ German Research Centre for Geosciences Section 4.6 Geomorphology, Telegrafenberg, 14473 Potsdam, Germany; Harald G. E. Fuchs, German Alpine Society, Section Berlin, Seydlitzstr. 1K, 10557 Berlin, Germany; Veronika Dirksen and Oleg Dirksen, Institute of Volcanology and Seismology FED RAS, Piipa blvd. 9, 683006 Petropavlovsk-Kamchatsky, Russia; Liudmila Syrykh, Herzen Pedagogical State University, Moika Embankment 48, 191186 Saint-Petersburg, Russia and Kazan Federal University, Kremlyovskaya str. 18, 420018 Kazan, Russia; Nadezhda G. Razjigaeva, Pacific Geographical Institute FEB RAS, Radio Street 7, 690041 Vladivostok, Russia;

received 17th February 2020, accepted 29th July 2021.

The Kamchatka Peninsula (eastern Russia) is one of the most remote and least studied regions of eastern Asia. It lies in the Russian Far East between the Sea of Okhotsk to the west and the North Pacific to the east (Fig. 1). The area experiences frequent tectonic, volcanic and cyclonic activities (Jones & Solomina 2015). This is one of the world's most volcanically and tectonically active regions, with active eruptions occurring in the Late Pleistocene between 45 and 39 ka ago and 30 and 25 ka ago and enhanced volcanic activity occurring in the Early to Middle Holocene between 9.5 and 7.0 ka BP (Ponomareva *et al.* 2007). The Pacific Plate is actively subducting beneath the Kamchatka Peninsula at about 80–100 mm a^{-1} resulting in three distinct volcanic arcs. There are about 300 volcanoes, more than 20 of which are active (Braitseva *et al.* 1997; Gledhill 2007; Jones & Solomina 2015) and include caldera, stratavolcanoes, somma-volcanoes and mixed types; additionally, there are many thermal and mineral springs and geysers.

The climate of Kamchatka is complex and influenced by the position of the Peninsula along the eastern margin of the Asian landmass, by cold ocean currents to the east and the Sea of Okhotsk to the west. Moreover, submeridional mountain areas with recent glaciation and permafrost yield steep climatic gradients, most pronounced between coastal and interior areas (Dirksen *et al.* 2013). Palaeoenvironmental records from this unique region are important for understanding of past climate and landscape changes and volcanic activity within Beringia (Lozhkin *et al.* 2011; Palagushkina *et al.* 2017; Subetto *et al.* 2017) and for evaluating its response to the modern climate warming (Kaufman *et al.* 2009; Brooks *et al.* 2015). Recent studies of palaeoclimate in Kamchatka confirmed a high degree of environmental variability between different parts of the peninsula and a mismatch in timing and magnitude of some Holocene climate events. Some delay of the HTM was observed at sites close to the Pacific Ocean relative to inland sites (Dirksen *et al.* 2013; Brooks *et al.* 2015). In central

DOI 10.1111/bor.12554

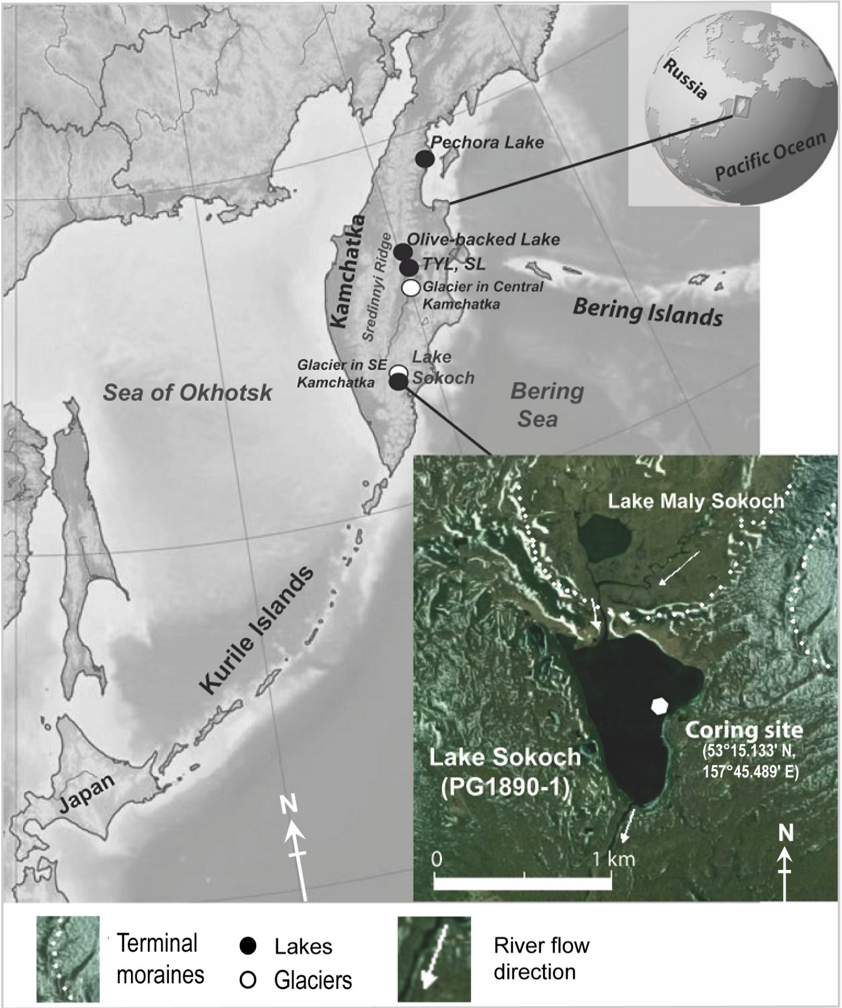

Fig. 1. Location of Lake Sokoch in Kamchatka (Russia) together with the other sites earlier studied in Kamchatka. Arrows show direction of the water-flow. [Colour figure can be viewed at www.boreas.dk]

Kamchatka, an expansion of birch and alder indicated warm, wet conditions associated with the HTM started from 8.9 cal. ka BP. In contrast, forest expansion in coastal regions did not start before 7.0 cal. ka BP (Dirksen *et al.* 2013). Neoglacial cooling started first in the northern parts of Kamchatka from 5.8 cal. ka BP, and from 5.0 cal. ka BP in central and coastal areas. The start of the Neoglacial in the south of Kamchatka is controversial (Brooks *et al.* 2015).

We investigated a Holocene sediment record from Lake Sokoch, southern Kamchatka. From this core, partly contradictory qualitative interpretation of diatom (Hoff *et al.* 2014) and pollen (Dirksen *et al.* 2015) data were obtained and published. A relatively warm period, corresponding to the HTM was reconstructed from both diatoms and pollen after 9.6 cal. ka BP. But the Neoglacial cooling, according to pollen data, started after 5.1 cal. ka BP and was evidenced by a pronounced forest retreat, while diatoms reflected a climate deterioration only after 2.7 cal. ka BP.

In this paper, we present new data derived from semi-aquatic (chironomids) and terrestrial (leaf wax biomarkers and their stable hydrogen isotope values) proxies from sediments of Lake Sokoch. Chironomids are well known as good indicators of air temperature and hydrological conditions (Stief *et al.* 2005; Engels *et al.* 2012, 2020; Heiri *et al.* 2014; Nazarova *et al.* 2017a, b). Long-chain *n*-alkane biomarkers, derived from the leaf waxes of higher terrestrial plants and their stable hydrogen isotope composition (expressed as a δ^2H or δD values) record hydrological change (Sachse *et al.* 2010, 2012; Kahmen *et al.* 2013). δ^2H values of the biomarkers depend on the isotope composition of precipitation, which can be influenced by temperature and evaporation as well as the moisture source (Gat 1996) and can be modified by plant evapotranspiration under arid conditions (Feakins & Sessions 2010; Sachse *et al.* 2010; Kahmen *et al.* 2013). As such, sedimentary records of leaf wax *n*-alkane δ^2H values have become powerful tools to reconstruct continental palaeohydrological changes over different time scales (Tierney *et al.* 2008).

The main aim of this study is to produce qualitative and quantitative reconstructions of the regional climate and limnological conditions during the Holocene using chironomid and biomarker records from Lake Sokoch. We compare our newly obtained results with earlier published inferences from pollen, diatoms and sediment chemistry records for this lake (Hoff *et al.* 2014; Dirksen *et al.* 2015) along with interpretations of the palaeoclimate from other parts of Kamchatka in order to bring our research into the broader regional context.

Material and methods

Study site

Lake Sokoch (LS) (latitude 53°15.133′N, longitude 157°45.489′E, altitude 495 m a.s.l.) lies at the southernmost tip of Ganal'sky Ridge, which belongs to the Eastern Ridges and borders the southern part of the central Kamchatka Depression between the Eastern Volcanic Zone and Pacific coast (Fig. 1). During the Last Glacial Maximum (LGM) *c.* 22–18 cal. ka BP, this area was relatively weakly glaciated (Braitseva *et al.* 1968). The nearest glaciers originated from large cirques that deposited two terminal moraines in the river valleys approximately 10 km from the modern glacier edge (Braitseva *et al.* 1968). LS is confined by the steep fronts of these moraines. The lake has a triangular form (1000×750 m in size) with a maximum water depth of 7 m. Morainic landforms bordering the lake and a U-shaped river valley with a roughly 2.5 by 1.5 km wide glacial cirque at the upper part of the valley prove the proglacial origin of the lake system (Fig. 1). The lake is a hydrologically open system with one major inflowing stream in the north and one outlet at its southern end. Approximately 500 m to the north of LS behind the lobate arc of younger moraine deposits there is another lake, Maly Sokoch (300 m in diameter; Fig. 1). It has a narrow channel connection to LS. The rounded basin of Lake Maly Sokoch is now ~300 m in diameter but it was apparently larger in the past, up to ~1600×1000 m in size (Hoff *et al.* 2014). This former lake area is now occupied by a wide shrubby bog (Dirksen *et al.* 2015).

The study area has a temperate continental climate with cold winters and cool summers. The mean January air temperature is −11.3 °C and the mean July temperature (T July) is 9.4 °C. The annual precipitation is 850 mm (www.iwmi.org). The lake lies within the zone of sub-alpine forest close to the upper limit of the tree line at 650–700 m a.s.l. and is surrounded by an open stone birch (*Betula ermanii*) forest with shrubs and short herbs in the understory (Dirksen *et al.* 2015).

Core lithostratigraphy

A 92-cm-long sediment core (PG1890-1) was obtained in September 2007 from 4.5-m water depth in the north-eastern part of LS (Hoff *et al.* 2014; Fig. 1). The sediments consisted mainly of light brown gyttja with the lowermost 8 cm represented by sandy gyttja. The core contains five layers of volcanic ash (1–5 cm thick; Fig. 2), consisting of well-sorted fine- to coarse-grained, light-coloured sand. A layer of poorly sorted material at the depth of 66–71 cm most probably is related to a mudflow that entered LS (Dirksen *et al.* 2015).

Except for the volcanic ash layers (1–5 cm thick), the sediment core was sliced in 1-cm intervals, freeze-dried and split into subsamples for micropalaeontological, sedimentological and stratigraphical analyses at AWI Potsdam. Results of diatom analysis and sedimentological data are presented in Hoff *et al.* (2014) and pollen data in Dirksen *et al.* (2015).

Radiocarbon dating and age model

Accelerator mass spectrometry (AMS) radiocarbon dating (^{14}C) was carried out at Poznán Radiocarbon Laboratory, Poland, on the total organic carbon fraction of eight sediment samples (Table S1). The ^{14}C dates were calibrated to calendar years before present (BP; 1950), by using the CalPal online program (Danzeglocke *et al.* 2010). Eight radiocarbon dates (Table S1) span the last *c.* 9.6 ka. The uppermost sample has a calibrated age of −0.026 cal. ka BP, indicating that reservoir effects possibly can be neglected in the interpretation of radiocarbon dates. The lowermost sample at 95 cm (core-catcher), corresponding to *c.* 9.4 cal. ka BP, has an Early Holocene age. Overlying sediments at 87 and 84 cm yielded ages of 9.6 and 8.86 cal. ka BP, respectively. The 'old' sample was omitted from interpolation of the age–depth relationship (Fig. 2), as it might include reworked older material (Hoff *et al.* 2014). In this paper we adopted the age model that has been developed in the previous study on LS (Hoff *et al.* 2014; Fig. 2).

Lake water and sediments chemistry

A single water-depth profile was taken in the centre of Lake Sokoch on 25th September 2007 (Hoff *et al.* 2014). The water-depth profile demonstrates a nearly uniform vertical distribution of temperatures between 10.8 and 11.1 °C and a low variability of the oxygen concentrations (7.3–7.7 mg L^{-1}, corresponds to an oxygen saturation of 66–69%). Lake water had low ion concentrations (total dissolved ions: 36.8–38.7 mg L^{-1}, conductivity: 45–46 mS cm^{-1}) and was slightly alkaline (pH 8.03–8.24), with the pH tending to increase towards the lake bottom. The ion composition, with $Ca^{2+}>Na^{+}>Mg^{2+}>K^{+}$ and $HCO^{3-}>SO_4^{2-}>Cl^{-}$, indicated a terrigenous origin of the water, supplied by river runoff and precipitation in an open lake system (Wetzel 2001).

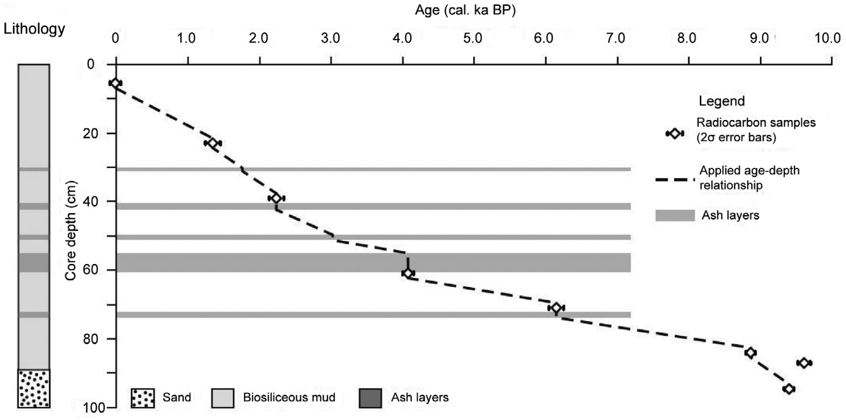

Fig. 2. Lithology and applied age–depth relationship of sediment sequence PG1890-1 from Lake Sokoch (adapted from Hoff *et al.* 2014).

Chironomid analysis

Treatment of sediment samples for chironomid analysis followed standard techniques described in Brooks *et al.* (2007). In order to capture the diversity of the chironomid communities that is necessary for a reliable estimate of inferred temperatures we extracted 54–117 chironomid larval head capsules from each sample (Larocque 2001; Quinlan & Smol 2001). Chironomids were identified to the highest taxonomic resolution with reference to Wiederholm (1983) and Brooks *et al.* (2007). Information on the ecology of chironomid taxa was taken from Brooks *et al.* (2007), Moller Pilot (2009; 2013) and Nazarova *et al.* (2008, 2011, 2015, 2017b, c); values of air temperature optima are taken from Nazarova *et al.* (2011, 2015).

Stratigraphical diagrams were created in C2 version 1.7.7 (Juggins 2007). Zonation of the chironomid stratigraphy was done using the optimal sum-of-squares partitioning method (Birks & Gordon 1985) using the program ZONE (Lotter & Juggins 1991). The effective number of taxa (Hill's N2 index; Hill 1973) were estimated after sample-size normalization using a rarefaction analysis in the iNext package version 2.0.20 (Chao *et al.* 2014; Hsieh *et al.* 2020) in R (R Core Team 2012).

To determine the lengths of the sampled environmental gradients, from which we decided whether unimodal or linear statistical techniques are the most appropriate for the data analysis, we performed detrended correspondence analysis (DCA), detrended by segments, on the chironomid data (rare taxa downweighted) (Birks 1995). DCA shows that the eigenvalues for DCA axes 1 and 2 are 0.445 and 0.179 and gradient lengths of species scores axes 1 and 2 are 2.75 and 2.165 standard deviation units, respectively, which implies that numerical methods based on a lineal response model are the most appropriate for assessment of the variation in structure of the chironomid assemblages (ter Braak 1995).

Principal component analysis (PCA) was used to explore the main pattern of variation of chironomids, biomarkers, diatoms and pollen data throughout the sediment core (ter Braak & Prentice 1988).

We reconstructed mean July air temperatures (T July) by using a Far East (FE) chironomid-based temperature inference model (Nazarova *et al.* 2015). The T July FE model has been previously used for palaeoclimatic inferences in the Russian Arctic, Siberia and Far East and demonstrated high reliability of the reconstructed parameters (Nazarova *et al.* 2013a, 2021a, b; Solovieva *et al.* 2015; Syrykh *et al.* 2017; Wetterich *et al.* 2018). Chironomid-based reconstructions were performed in C2 version 1.5 (Juggins 2007). The data were square-rooted to stabilize species variance.

To assess the reliability of the chironomid-based reconstruction, we calculated percentage abundances of the taxa that are absent or rare in the modern calibration data sets. Less reliability was placed on the samples in which more than 5% of taxa were not represented in the modern calibration data or more than 5% of taxa were rare in the modern calibration data set (i.e. Hill's N2 less than 5; Heiri & Lotter 2001; Self *et al.* 2015; Plikk *et al.* 2019). Goodness-of-fit statistics derived from a canonical correspondence analysis (CCA) of the modern calibration data and down-core passive samples with T July as the sole constraining variable (Birks *et al.* 1990; Heiri & Lotter 2001; Palagushkina *et al.* 2012; Frolova *et al.* 2013). This method shows how unusual the fossil assemblages are in respect to the composition of the training set samples along the gradient of interest. Fossil samples with a residual distance to the first CCA axis larger than the 90th and 95th percentiles of the residual distances of all the modern samples were identified as samples with a 'poor fit' and a 'very poor fit' with T July, respectively (Birks *et al.* 1990).

DCA, PCA and CCA were performed using CANOCO 4.5 (ter Braak & Šmilauer 2002). Chironomid percentage data were square-root transformed and rare taxa were downweighted.

Biomarker analysis

For biomarker extraction between 0.52 and 4.90 g of dry sediment was used. To obtain a total lipid extract (TLE) we used a Dionex accelerated solvent extraction system (ASE 350) with a 9:1 dichloromethane (DCM):methanol (MeOH) mixture (9:1) operated at 100 °C and 103 bar for 15 min in two cycles following established laboratory protocols of the Helmholtz Centre Potsdam GFZ German Research Centre for Geosciences. To the TLE an internal standard (5α-androstane) was added. The TLE was separated into two fractions (aliphatic compounds, F1 and polar compounds F2) by solid phase extraction (SPE) using 2 g silica gel as the stationary phase and hexane and DCM:MeOH (9:1) as the respective mobile phases. The F1 fraction was passed over activated copper in a pipette column to remove elemental sulphur, the F2 fraction was archived.

The chromatographic analysis of the *n*-alkanes (dissolved in hexane) was done with a 30-m DB-5MS UI column (diam. 0.250 mm, film 0.25 μm). The compound identification was done in a two-step procedure: first by using a NIST mass spectra library and second by comparing sample *n*-alkane retention times to an external C10 to C40 *n*-alkane standard, which was measured at the beginning of each sequence. The GC temperature program began with sample injection at 70 °C (held for 3 min), then heating up to 320 °C with a ramp of 8 °C per minute. The final temperature of 320 °C was held for 30 min. The PTV injector started at 70 °C and was heated to 320 °C with a ramp of 12 °C per second.

In order to obtain sufficient material for compound-specific stable isotope measurements, we combined three consecutive samples (four consecutive samples for the lowermost sample) into one, resulting in eight samples. δ^2H values were measured on the nC_{23}, nC_{25}, nC_{27}, nC_{29} and nC_{31} alkanes. Compound-specific hydrogen isotope ratios (δ^2H or δD values) of the F1 fraction were measured using a Delta V Plus Isotope Ratio Mass Spectrometer (IRMS; Thermo Scientific, Bremen, Germany) coupled to a Trace 1310 GC (with an Agilent DB-5 column, 30 m×0.25 m×0.25 μm film) via a Thermo GC Isolink pyrolysis furnace operated at 1420 °C. Every sample was measured in duplicate. Correction of δ^2H values to the VSMOW scale was done using a linear regression function derived from the relationship of an *n*-alkane standard mixture (Mix A4, supplied by Arndt Schimmelmann, Indiana University, USA) with known δD values to its measured values. The $H3^+$ factor was determined once a day and had stable a value of 2.4, indicating stable ion source conditions.

Results

Chironomids

In total, we identified 70 chironomid taxa, most of which had only single occurrences. Only 21 taxa had N2 above 5 and were non-rare. Chironomid communities are strongly dominated by two *Corynocera* taxa: *C. ambigua* dominate until 3.0 cal. ka BP, and *C. oliveri*-type thereafter. An unusual structure of chironomid communities is reflected by diversity indices.

PCA 1 (Fig. 3) explains 55% of the total variance of chironomid data and high axis scores correlate with high abundances of *C. ambigua*. The low scores of PCA 1 correlate with *C. oliveri*-type. Both taxa are cold stenotherms, but *C. oliveri*-type has lower T July optima in all Russian models (Nazarova *et al.* 2011, 2015) and was found in colder sites than *C. ambigua* in a northwest North American training set (Barley *et al.* 2006). The second PCA axis explains 13.3% of the variance within the data set and high axes scores correlates with high abundances of phytophilic taxa (*Paratanytarsus austriacus-type, Cricotopus laricomalis-type, Phaenopsectra flavipes-type, Psectrocladius sordidellus-type. Psectrocladius barbimanus-type).* Low scores for PCA 2 correlate with profundal taxa *Tanytarsus lugens-type* and *Micropsectra insignilobus-type* (Fig. 3). Correlation of high and low scores of PCA 1 and 2 with these ecological groups of chironomids shows that PCA 1 mainly reflects changes in temperature. The chironomid record is divided into six chironomid assemblage zones (CH I–VI, Fig. 3).

CH I (9.4–9.0 cal. ka BP). – In the lowermost zone, *C. ambigua* has a median abundance of 63%. Several littoral taxa tolerant to meso- and eutrophic conditions and often associated with macrophytes have abundances up to 10%: *Cladotanytarsus mancus-type, Dicrotendipes nervosus-type, M. insignilobus*-type, *Stictochironomus* and *Tanytarsus pallidicornis-type.* Among them, *C. mancus*-type and *Stictochironomus* can occur in both lotic and lentic environments. Acidophobic *M. insignilobus*-type declines to 5% at 9.0 cal. ka BP in line with an increase of *C. ambigua* and other phytophilic, acidophilic and eutrophic taxa. Reconstructed T July are ~1 °C above modern level (median 10.4 °C).

CH II (9.0–6.4 cal. ka BP). – Phytophilic taxa decrease or disappear. Chironomid diversity (N2) strongly declines. Together with the very high abundances of *C. ambigua* in this zone we observe a steady increase of taxa tolerant to anoxic conditions *Procladius* has the highest abundance at *c.* 7.1 cal. ka BP and reduces to 2% thereafter. At the same time, *M. insignilobus*-type appears again in the lake and its abundances gradually rise. Reconstructed T July are on average 1 °C warmer

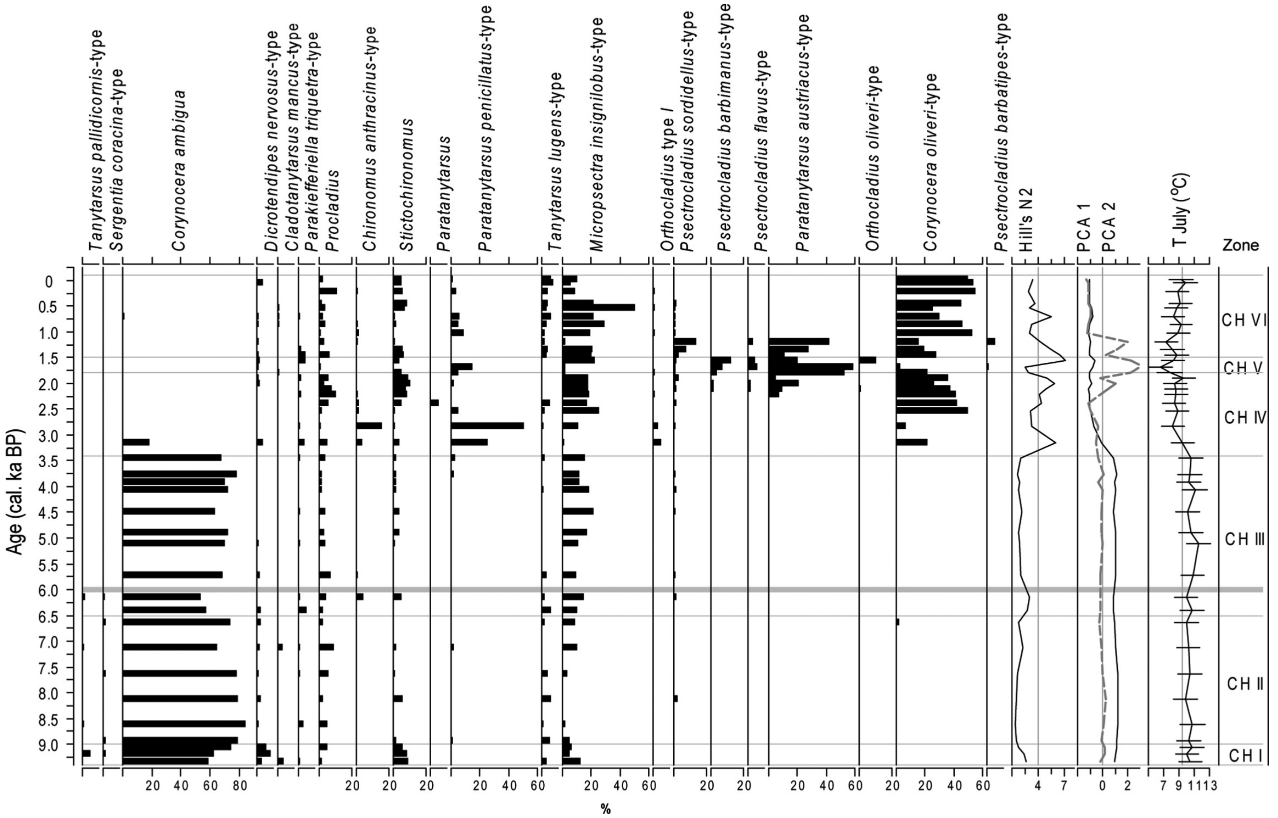

Fig. 3. Relative proportions of 'non-rare' chironomid taxa (N2 > 5) in the sediments of Lake Sokoch, Hill's N2, chironomid-inferred T July and PCA axes 1 and 2 scores for chironomid data.

than today (median 10.3 °C) with a small cooling spell (9.8 °C) around 8.2 cal. ka BP.

CH III (6.4–3.4 cal. ka BP). – Between 6.4 and 6.0 cal. ka BP, taxonomic diversity increases (Fig. 3). Abundance of *C. ambigua* decreases and we observe a short increase in littoral phytophilic *Paratanytarsus*, *Parakiefferiella triquetra* type, and the profundal taxa *Chironomus anthracinus* type, *Stictochironomus* and *T. lugens* type. *M. insignilobus*-type reaches highest abundances between 4.5 and 4.0 cal. ka BP. After 6.0 cal. ka BP abundances of *C. ambigua* increase. Reconstructed T July remain on average 1 °C above modern level, with the warmest period between 6.0 and 5.0 cal. ka BP when the reconstructed T July are 2 °C warmer than today (11.5 °C).

CH IV (3.4–1.8 cal. ka BP). – *C. ambigua* declines after 3.4 cal. ka BP and we observe a rise in diversity of chironomid communities. Between 3.2 and 2.5 cal. ka BP, *P. penicillatus*-type and *C. anthracinus*-type have the highest abundances in the whole record. These taxa prefer colder conditions, are associated with macrophytes and tolerant to low oxygen and low pH. Reconstructed T July decrease to 1.2 °C below modern level (8.2 °C).

After 2.5 cal. ka BP, *C. anthracinus*-type and *P. penicillatus*-type are replaced by *C. oliveri*-type, *M. insignilobus*-type, *Stictochironomus* and *Procladius.* Abundances of the cold stenotherm *P. austriacus*-type increase. Reconstructed T July are ~1 °C below modern level (8.4 °C).

CH V (1.8–1.5 cal. ka BP). – During this short period, we observe another abrupt faunal change. All taxa that dominate the previous zone strongly decline or disappear. Chironomid communities are composed of cold stenotherm *P. austriacus*-type, *P. penicillatus*-type, *P. triquetra*-type, and acidophilic *Psectrocladius* taxa. Chironomid diversity and reconstructed T July strongly decrease (up to 6.6 °C).

CH VI (1.5 cal. ka BP–present). – *C. oliveri*-type and *M. insignilobus*-type dominate the upper part of the core. *P. austriacus*-type and *P. penicillatus*-type decline, and *P. penicillatus*-type disappears after 1.1 cal. ka BP. *T. lugens*-type and *Procladius* are constantly present. *P. sordidellus*-type has a maximum around 1.1 cal. ka BP and nearly disappears from the lake thereafter. Reconstructed T July rise and reach modern level (9.4 °C) in the uppermost samples.

Quality of T July reconstruction

Nineteen of 70 identified chironomid taxa are rare in the FE data set and five taxa are absent. Of these rare and absent taxa, only *P. triquetra*-type and *Micropsectra radialis-type* reach abundances of 4% (Fig. 3) in the core.

Goodness-of-fit statistic reveals that 8 of 48 samples have a 'very poor fit' and 11 had a 'poor fit' with T July (Fig. S1). Samples from the lower horizons of CH V (*c*. 1.9–1.78 cal. ka BP) have the worst fit with T July. However, there is little empirical evidence of the relationships between 'fit' of fossil and training-set samples and increased error or unreliability if fossil taxa are well represented in the training set (Juggins & Birks 2012). Experiments with simulated data suggested that methods, apart from the modern analogue technique, perform well under moderate non-analogue situations (ter Braak *et al*. 1993; ter Braak 1995). Reconstructions for such samples should probably be treated with caution, although when most of the taxa in the fossil samples are present in the training set, there are no reasons for suspecting the reconstructions to be an error (Juggins 2001). Therefore, although the representation of the fossil taxa in the FE T July data set are good, results for the GoF statistic suggest that T July reconstruction for the parts of the core with 'very poor fit' should be probably treated with caution and should be supported by results obtained from the other available proxy.

Biomarkers

In the sediment extracts, we identified *n*-alkane biomarkers of variable chain length, ranging from $n\mathrm{C}_{17}$ to $n\mathrm{C}_{33}$. All samples are characterized by a strong odd over even carbon number predominance. The overall concentration of *n*-alkanes is relatively low, with maximum values of 9.04 μg g^{-1} sediment. The most abundant *n*-alkane in almost all samples is $n\mathrm{C}_{27}$ with concentrations ranging from 0.32 to 9.04 μg g^{-1} sediment, followed by $n\mathrm{C}_{29}$, $n\mathrm{C}_{25}$ and $n\mathrm{C}_{31}$ with concentrations ranging from 0.20 to 5.82 μg g^{-1} sediment (Fig. 4). Short-chained *n*-alkanes, such as $n\mathrm{C}_{17}$ and $n\mathrm{C}_{19}$ are present in some samples in the upper 10 cm of the core (*c*. 0.25 cal. ka BP; due to low concentration they are not shown in Figs 4 and S2). Mid-chain *n*-alkanes, such as $n\mathrm{C}_{21}$ and $n\mathrm{C}_{23}$, are present throughout the core in lower concentrations ranging from 0.11 to 1.91 μg g^{-1} sediment. In general, all biomarker compounds remain in very low concentrations below *c*. 2.3 cal. ka BP but show substantially higher concentrations thereafter (Fig. 4).

δ^2H values of the $n\mathrm{C}_{23}$ and $n\mathrm{C}_{25}$ alkanes range from −202 to −209 and −200 to −215‰, respectively. The $n\mathrm{C}_{31}$ alkanes range from −199 to −207‰, whereas δ^2H values of the $n\mathrm{C}_{27}$ and $n\mathrm{C}_{29}$ alkanes range from −216 to −225 and −213 to −220‰, respectively. In general, all *n*-alkane biomarkers show a pronounced decrease of δ^2H values of about 10–15‰ after *c*. 2.3 cal. ka BP (Fig. 4).

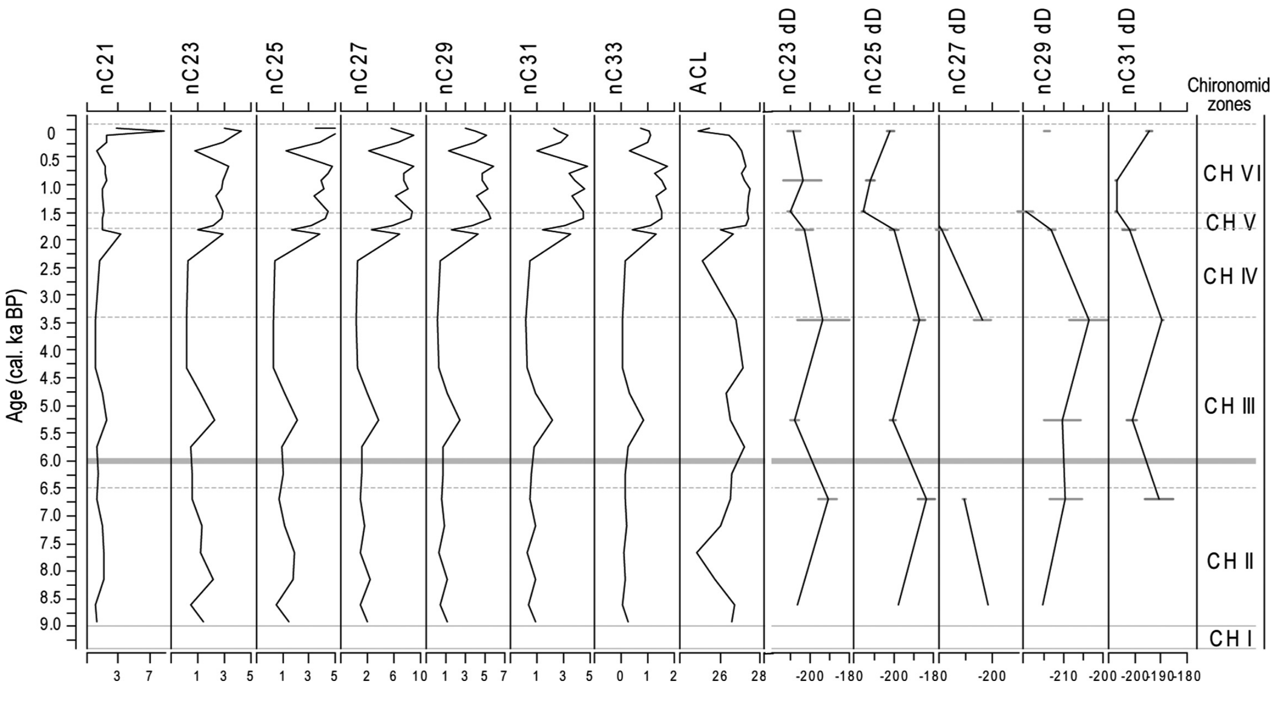

Fig. 4. Down-core variation of biomarker data. Dashed lines differentiate chironomid assemblage zones I to VI (CH I–VI).

Discussion

The sediment core from LS provides a Holocene palaeoecological record for the southern part of central Kamchatka. Several stages in lake development and evolution of the environment can be recognized from changes in fossil chironomid communities (Fig. 3) and biomarker records (Fig. 4) discussed herein, together with the results of diatom, sediment composition and pollen analysis (Figs 5, S3) (Hoff *et al.* 2014; Dirksen *et al.* 2015).

Variations in the investigated proxy (Fig. 5) suggest that palaeolimnological changes to some extent were driven by climatic changes.

The lowermost interval of the sediment core documents the onset of lacustrine conditions in the lake, possibly related to local glacier retreat during the Early Holocene. Between 9.6 and 9.0 cal. ka reconstructed T July were ~1 °C above modern level (Figs 3, 5). The chironomid fauna was dominated by littoral meso- and eutrophic taxa, some of which were characteristic of lotic environments and could be brought in with melting water from the upstream glaciers (Fig. 3). Cold-stenotherm acidophobic *M. insignilobus*-type (Nazarova *et al.* 2015) is gradually replaced by *C. ambigua* and several phytophilic chironomid taxa suggesting spreading of macrophytes in the initially shallow lake under relatively warm climatic conditions. Low overall concentrations of terrestrial and aquatic biomarkers (Fig. 4), as well as low amounts of biogenic opal, and organic carbon in the lowermost sediment layer (Fig. S3) point to low biological productivity at the beginning of the record (*c.* 9.4 cal. ka BP) that rose towards 9.0 cal. ka BP as indicated by the increasing trend of C:N ratio, S, total organic carbon (TOC), δ^{13}C and biogenic opal (Figs 5, S3) (Hoff *et al.* 2014). This is further supported by the presence of periphytic/benthic diatoms (Hoff *et al.* 2014) and growing abundances of green algae (*Botryococcus*, *Scenedesmus*, *Tetraedron minimum* and *Pediastrum*) that develop under meso- to eutrophic conditions (Dirksen *et al.* 2015). High abundances of *Botryococcus* that prefer stagnant and shallow water bodies (Guy-Ohlson 1992;

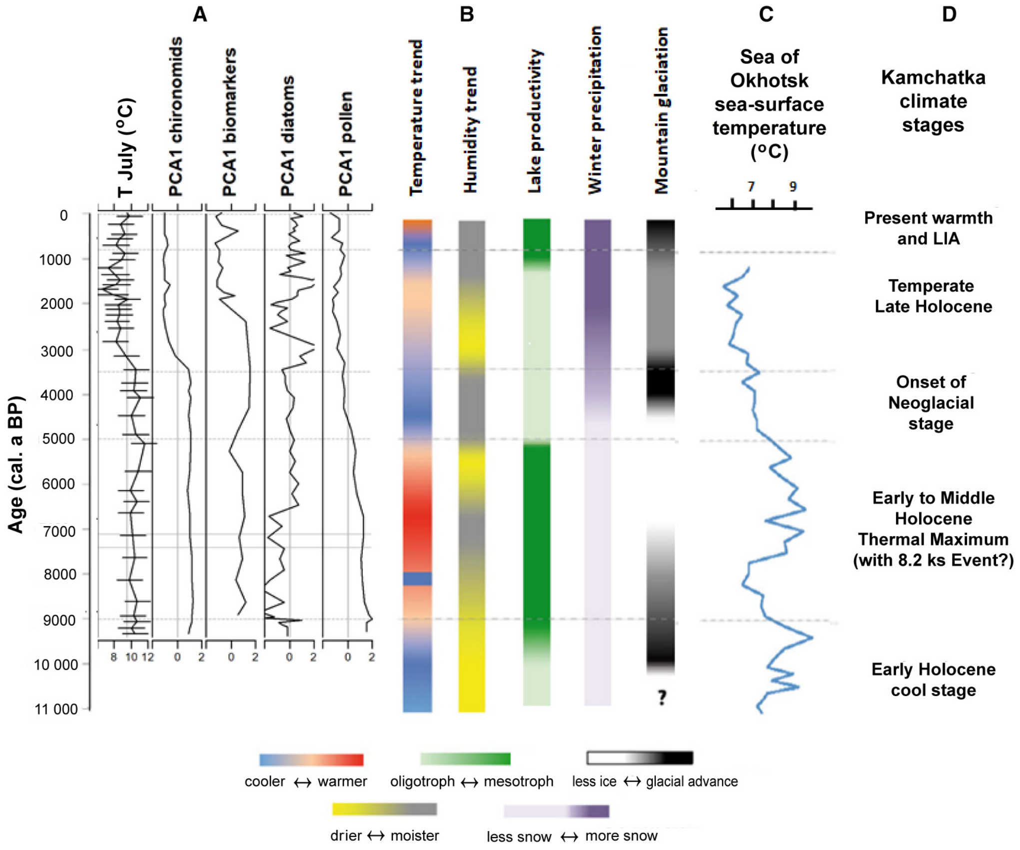

Fig. 5. Compilation of palaeoenvironmental interpretations of the Kamchatka palaeoenvironment for the Holocene. A. Down-core variations of sediment core PG1890-1: chironomid-inferred T July (°C); PCA 1 of chironomid, biomarker (present study), diatom (Hoff *et al.* 2014) and pollen data (Dirksen *et al.* 2015). B. Trends in temperature, humidity changes in lake trophy inferred from lake records of Kamchatka (Andrén *et al.* 2015; Dirksen *et al.* 2015; Hoff *et al.* 2015; Self *et al.* 2015; Solovieva *et al.* 2015), trends in winter precipitation inferred from vegetation dynamics and stable isotope signals in lake records of Kamchatka (Hammarlund *et al.* 2015; Meyer *et al.* 2015), and timing of mountain glaciation on Kamchatka (Barr & Solomina 2014; Meyer *et al.* 2015). C. Alkenone-based sea-surface temperature reconstructions in the Sea of Okhotsk at Site LV29-114-3 (Max *et al.* 2012). D. Kamchatka climate stages (Brooks *et al.* 2015). [Colour figure can be viewed at www.boreas.dk]

Riera *et al.* 2006) prove that shallow conditions existed in the initial stage of lake development (Hoff *et al.* 2014).

The presence of lotic chironomid taxa, low concentrations of terrestrial and aquatic biomarkers, dominance of small periphytic/benthic diatoms, and rise of biological productivity indicate a changing environment (Lotter & Biegler 2000; Biskaborn *et al.* 2019) in and around the newly developing lake ecosystem. In the valleys neighbouring LS, morainic relics of Lateglacial retreat were dated at *c.* 10.0 cal. ka BP (Savoskul 1999). Thus, the formation of LS can be seen in association with the onset of the Early Holocene climate warming in the interior of the peninsula and an increase of meltwater runoff due to glacial retreat. The postglacial warming of sea-surface temperatures at the northeast Pacific margin of Kamchatka took place earlier, at *c.* 11.0 cal. ka BP (Max *et al.* 2012; Brooks *et al.* 2015) and had an environmental impact at least 1000 years later at the higher elevation of southern Kamchatka (Fig. 5).

From 9.0 until 3.0 cal. ka BP chironomid communities were represented mainly by *C. ambigua*, a brachypterous taxon that might have been able to avoid the hazards of flight in windy conditions and is among the first immigrants to lakes following glacial retreat in Europe (Berglund & Digerfeldt 1970; Hofmann 1978, 1983a, b; Schakau & Frank 1984; Brodin 1986). The adults can be carried long distances by thermal convection and turbulent air masses (Walker & Mathewes 1988). In the study lake this taxon was able to develop dense populations under environmental conditions unfavourable for swarming of winged chironomid taxa and declined when conditions became less turbulent and other chironomid taxa became able to swarm and reproduce.

Shallow limnic conditions and high production of aquatic macrophytes from near-shore areas and/or higher land plants between 9.0 and 8.0 cal. ka BP are suggested by peaks in mid-chain *n*-alkanes (nC_{23}) (Ficken *et al.* 2000) and a relatively high C:N ratio (Meyers & Teranes 2001) (Figs 4; S3). Planktonic diatom taxa strongly declined and diatom assemblages were dominated by tychoplanktonic species (Hoff *et al.* 2014) – free-living or attached benthic species that get into plankton through a disturbance of their benthic habitat, or by winds and currents.

Reconstructed T July remained on average 1 °C warmer than today with a short weak cooling around 8.2 cal. ka BP. This cooling is as well supported by some decline of white birch (*Betula platyphylla*) forest along with downy alder (*Alnus hirsuta*) forest that is observed around 8.0 cal. ka BP (Dirksen *et al.* 2015). Although evidence of the well-known 8.2 ka cooling event is mostly found in North Atlantic regions (Alley *et al.* 1997; Kerschner *et al.* 2006; Nazarova *et al.* 2020), some sites in Kamchatka provide evidence of this event as well. In the south of Kamchatka (Topolovaya Valley), moraine sequences reflect a former presence of glaciers at *c.* 8.5 cal. ka BP (Savoskul & Zech 1997). Similar evidence was found 100–150 km north of the Topolovaya Valley, in the headwaters of the Sredniya Avacha River (Savoskul 1999). Glacial advances were found in central Kamchatka (Klyuchevskaya group of glaciers) starting prior to 8.5 cal. ka BP (Yamagata *et al.* 2000, 2002). At the Bilchenok and Koryto sites (central Kamchatka), glacial advance is dated at *c.* 8.3 cal. ka BP. At the West Ichinsky site, the till layer was found beneath the tephra *c.* 7.8 cal. ka BP (Barr & Solomina 2014). In northeast Kamchatka (Andrén *et al.* 2015), both the pollen and diatom records indicate a brief cooling at *c.* 8.2 cal. ka BP, and a short, dry period at around 8.0 cal. ka BP was indicated in pollen records elsewhere in Kamchatka (Fig. 5) (Dirksen *et al.* 2013).

We suppose that cooler and drier conditions led to reduction of meltwater inflow from the glaciers causing short-term shallowing of the lake that terminated around 8.2 cal. ka BP. Decrease of the mid-chain *n*-alkane (nC_{23}) concentration and C:N ratio after *c.* 8.2 cal. ka BP indicated reduction of the allochthonous input of organic matter into the lake (Meyers & Teranes 2001). Further lowering of the lake level, and consequently, shrinking of the macrophyte belt at the lake littoral is supported by taxonomic shifts in chironomid and diatom communities. Dominance of brachypterous *C. ambigua* and tychoplanktonic diatoms suggests that lake conditions were disturbed during this time interval, probably by windy conditions, which can be especially noticeable in shallow limnic settings. Diatoms and sedimentary data indicate a shallow lake until *c.* 6.0 cal. ka BP (Hoff *et al.* 2014).

The C:N ratio showed a minimum point at *c.* 7.6 cal. ka BP (Fig. S3) indicating that the depositional environment was dominated by the accumulation of biogenic autochthonous material, mostly from pelagic algae (Hoff *et al.* 2014). At 7.4 cal. ka BP, acidophobic *M. insignilobus*-type appeared again, which together with high amounts of the tychoplanktonic diatoms *S. venter*, *S. mutabilis* and *S. martyi* suggested that the water conditions probably became alkaline. Taking into account the high representation of meso- to eutrophic diatom species (*A. subarctica*, *S. minutulus*, *S. venter*, *S. mutabilis* and *S. construens*), maximal abundance of green algae *Scenedesmus* and *Pediastrum* (Dirksen *et al.* 2015) and peaking of eurytopic, meso-to eutrophic *Procladius* (tolerant to anoxic conditions) at 7.1 cal. ka BP, we assume that this was an interval of shallow mesotrophic conditions under a mild climatic setting. A rise in the C:N ratio thereafter indicates an increase in surface runoff, in response to climate amelioration that is further supported by an increase in planktonic diatom species, particularly of *A. subarctica* that peaked at 7.1 cal. ka BP (Hoff *et al.* 2014).

Between 6.4–3.4 cal. ka BP an increase in $\delta^{13}C$ values of organic matter (Hoff *et al.* 2014) indicates a rise in palaeoproductivity, which together with lower C:N values indicate a change in the source of organic matter with a greater algal contribution and deepening of the lake. A deeper lake, and less disturbed limnic conditions under a steady warming climatic trend between 6.4 and 6.0 cal. ka BP are supported by a shift in diatom communities, as reflected by PCA 1 scores (Fig. 5). *Stephanodiscus* and *Aulacoseira* that thrive in turbulent water bodies decline and eutrophic *Staurosiramartyi* increase. Deepening of the lake caused by humidification of the climate is reflected by pollen data (Dirksen *et al.* 2015). Appearance of suitable shallow-water sites, likely due to higher lake levels and shore flooding after 6.4 cal. ka BP, was confirmed by the development of local wetlands with sedges and *Filipendula* and distribution of *Thelypteris palustris* and *Isoetes* (Dirksen *et al.* 2015).

Around 6.0 cal. ka BP, sediments included 5-cm-thick traces of a mudflow (Figs 3, 4). The reconstructed warming after 6.4 cal. ka BP in association with high precipitation (Dirksen *et al.* 2015) may have intensified melting of glaciers and snowfields in surrounding mountains, resulting in an increased water inflow. Considering the morphology of the catchment areas of LS and Lake Maly Sokoch (Fig. 1), we assume that the melting water from the upstream ridges first filled out the basin of Lake Maly Sokoch and then, by infiltration through and even by periodical pouring over the moraine arc. The mudflow could have been caused by a massive discharge of the meltwater stored in the Lake Maly Sokoch basin when its moraine gave way to a glacial outburst flow (Hoff *et al.* 2014). This event coincided with the warmest interval when the reconstructed T July averaged 2 °C above modern level (Figs 3, 5).

After 5.0 cal. ka BP high abundances of acidophobic and profundal *M. insignilobus-type,* and higher abundances of planktonic diatoms and diatoms indicative of more eutrophic conditions (*A. subarctica f. recta* and *S. alpinus*) could be explained by strengthened nutrient influx, which is supported by the increasing values of the C:N ratio and high values of $\delta^{13}C$ (Fig. S3). More humid conditions and eutrophic to hypertrophic water conditions can be inferred from the occurrence of *Stephanodiscus medius*, which is strictly limited to this interval (Cremer *et al.* 2007; Rioual *et al.* 2007; Hoff *et al.* 2014).

The interval between 4.0 and 3.4 cal. ka BP is bordered by two ash layers. Sedimentation rates had two peaks directly before and after the ash layers (Hoff *et al.* 2014). Chironomids demonstrated no clear response to the ashfalls, while the diatom diversity decreased and diatom PCA 1 suggested a noticeable taxonomic shift at 4.0 cal. ka BP. Ashfall-related, short-lived fluctuations in pollen, diatom and chironomid assemblages were observed earlier in some lakes in central and northern Kamchatka (Self *et al.* 2015; Solovieva *et al.* 2015).

The interval between 6.5 and 3.4 cal. ka BP can be attributed to the HTM with the warmest phase between 6.0 and 5.0 cal. ka BP. The glacial history of Kamchatka suggests the absence of any glacial advances in the area of investigation between 6.0 and 4.3 cal. ka BP (Savoskul 1999). The pollen record from LS suggested that forests were at their maximum extent between 7.4 and 5.1 cal. ka BP (Dirksen *et al.* 2013).

Pollen records from the Pacific coast document earlier maximum humidity and warmth, between 8.0 and 5.0 cal. ka BP (Fig. 5; Dirksen *et al.* 2013). The sediment records in central Kamchatka as well indicated a relatively warm climate until about 5.0 cal. ka BP and expansion of birch and alder from 8.9 to 5.0 cal. ka BP (Self *et al.* 2015).

During the warmer HTM climatic conditions, many lakes in Kamchatka became more productive. From 6.2 cal. ka BP, LS became increasingly nutrient-enriched under warm climatic conditions. Similar nutrient-enriched conditions were also apparent at the lakes in the highlands of central Kamchatka (Hammarlund *et al.* 2012) and on the northern Pacific coast of Kamchatka (Andrén *et al.* 2015; Solovieva *et al.* 2015). Chironomid-inferred temperatures there reached a peak between 5.7 and 5.3 cal. ka BP. Evidence for increased summer temperatures at this time has been found in other records in the region (Mayewski *et al.* 2004; Nazarova *et al.* 2013a).

After 5.0 cal. ka BP, the chironomid-inferred T July demonstrated a cooling trend. At the same time, δ^2H values of lipid biomarkers started to decline (Fig. 4), for example, the most abundant terrestrial biomarker nC_{27} showed a decrease in values from −203 to −218‰. In response to the beginning of the climatic cooling, stone birch forests near the lake retreated significantly between 5.1 to 3.5 cal. ka BP, and sub-alpine-like meadows and alder shrubland advanced, suggesting a lowering of the timberline (Dirksen *et al.* 2015). A remarkable disappearance of *T. palustris* and *Isoetes*, and abrupt decline of *Filipendula* indicated degradation of wetlands that can be explained by the river outflow from LS leading to the establishment of an open lake system and a steady decrease in lake level after 5.0 cal. ka BP.

At 3.4 cal. ka BP the strongest taxonomic shift in chironomid communities and diatom assemblages was observed (Fig. 5). Chironomid *C. oliveri*-type gradually replaced *C. ambigua*. Relatively little is known about the ecological preferences of *C. oliveri*-type and the ecology of *C. ambigua* is still debated (Brodersen & Lindegaard 1999; Halkiewicz 2009; Nazarova *et al.* 2013a). Oliver & Roussel (1983) suggested that *C. ambigua* inhabited predominantly cold lakes and ponds. Wiederholm (1983) attributed *C. ambigua* to Palaearctic and Nearctic lakes. *C. ambigua* has mainly been described as a cold-stenotherm species living in the sediments of shallow, oligotrophic lakes of arctic and sub-arctic regions (Fjellberg 1972; Pinder & Reiss 1983; Walker & Mathewes 1988), although it was also found in Lateglacial sediments of temperate lakes, often in very high numbers (Brodersen & Lindegaard 1999). In areas located more to the south, it was considered as a postglacial relict (Reiss & Gerstmeier 1984). These facts denote that ecological adaptations of *C. ambigua* are complex. But a sharp change in the distribution of *Corynocera* species that occurs at the tree line in Northern Yakutia (Russia) suggested that the distribution of *Corynocera* taxa may provide valuable palaeoclimatic information. *C. ambigua* in this region was found in warmer, forested sites, whereas *C. oliveri*-type dominates colder sites north of the tree line (Porinchu & Cwynar 2000). In the FE and Northern Russian (NR) inference models (Nazarova *et al.* 2015), these two *Corynocera* taxa demonstrated a clear difference in the T July optima. In the FE model, the T July optimum for *C. ambigua* is 10.0 °C and for *C. oliveri*-type, it is 8.8 °C. A similar difference was observed in the North Russian (NR) data set and inference model: 13.3 and 10.7 °C, respectively. Available ecological information on both of these dominant chironomid taxa supports the quantitatively reconstructed climatic change. The revealed strong taxonomic shift with the clear change of dominants from the less cold-tolerant *C. ambigua* to the cold-stenotherm *C. oliveri*-type in chironomid communities after 3.4 cal. ka followed the climatic deterioration and onset of Neoglacial cooling with the reconstructed T July ~1 °C below modern level. From 2.2 cal. ka BP, an increase of abundances of cold stenotherm *P. austriacus*-type indicated further cooling that culminates between 1.7 and 1.6 cal. ka BP.

Climate deterioration after 3.4 cal. ka BP was documented as well by a change in diatom assemblages (Hoff *et al.* 2014) and was supported by frequent glacier advances between 3.2 and 2.8 cal. ka BP in the wider vicinity of LS (Savoskul 1999). Although Neoglacial cooling in the north of Kamchatka started at *c.* 5.8 cal. ka BP and in central and coastal areas at *c.* 5.0 cal. ka BP (Brooks *et al.* 2015), radiolarian data from the Sea of Okhotsk, west of Kamchatka (Itaki & Ikehara 2004), suggested an onset of Neoglacial climate cooling between 3.3 and 2.4 cal. ka BP. A shift to drier climate and moderately cool conditions (Dirksen *et al.* 2015) between 3.5 to 2.2 cal. ka BP was evident from an advance of white birch forest at lower elevations alongside the stable relationship between stone birch forest and alder thickets surrounding the lake (Dirksen *et al.* 2015). Drier conditions are evident from the shallow state of LS until 2.5 cal. ka BP indicated by an appearance of macrophytes, Cladocera and shore wetlands (Dirksen *et al.* 2015), and a decrease of planktonic diatoms.

The interval between 3.4 and 1.8 cal. ka showed higher sedimentation rates and a stable diatom community of medium diversity. The C:N ratio showed a minimum, indicating limnic origin of organic matter, while the other parameters present small maxima. Between 2.2 and 1.7 cal. ka BP, the second maximum of stone birch occurred in the study area (Dirksen *et al.* 2015) pointing to a rise of the timberline. At this interval, *C. oliveri*-type declined while more eutrophic *Procladius* and two other cold stenotherm oligotrophic to mesotrophic chironomid taxa *Stictochironomus* and *P. austriacus-type* increased. High abundances of the taxa that can withstand low-oxygen conditions and pH fluctuations may be indicative of prolonged winter ice cover, as was suggested for the Two-Yurts Lake in central Kamchatka at this time (Nazarova *et al.* 2013a; Brooks *et al.* 2015). The reconstructed T July showed a short-term increase by 1 °C around 1.9 cal. ka BP.

Although some records across Kamchatka indicated climate amelioration between 2.5 and 1.1 cal. ka BP (Nazarova *et al.* 2013a; Brooks *et al.* 2015; Hoff *et al.* 2015; Meyer *et al.* 2015), evidence for cool and oceanic conditions at this time is also available from southwestern (Klimaschewski *et al.* 2015) and northern Kamchatka (Solovieva *et al.* 2015).

Near LS in the southeast of Kamchatka, two glacier advances were dated at 2.6–2.1 and 1.8–1.4 cal. ka BP, which is in accordance with chironomid, diatom and pollen data from LS suggesting a cool climate during these intervals with some short-lived amelioration in-between.

Between 1.8–1.5 cal. ka BP chironomid and diatom communities demonstrated another strong shift in taxonomic composition (Figs 3, 5). Reconstructed T July dropped significantly. Although the GoF tests and sum of rare taxa showed that the reconstructed T July for the upper part of the record were not fully reliable, the highest recorded abundances of cold-stenotherm *Orthocladius oliveri-type* (T July optima in the FE model 8.1 °C), and especially of *P. austriacus*-type (T July optima in the FE model 3.7 °C), and increased concentration of chrysophyte cysts (Hoff *et al.* 2014) pointed clearly to climatic deterioration. This short-term climatic cooling was reconstructed from several sedimentary records in central Kamchatka (Nazarova *et al.* 2013a, 2017a) and fits with glacial advances that occurred around 1.8–1.4 cal. ka BP (Savoskul 1999). An abrupt cooling under relatively dry conditions could lead to deterioration of water inflow into the lake and cause strong, short-lived drops in water level. At this time, higher abundances of periphytic/benthic species, decrease of tychoplanktonic species and low concentration of planktonic species (Hoff *et al.* 2014) support the short and abrupt shallowing of the lake.

After 1.5 cal. ka BP the reconstructed T July had variations but demonstrated a steady increasing trend towards modern time. From 1.5 to 1.3 cal. ka BP, disappearance of cold-stenotherm *P. austriacus*-type indicated climatic amelioration. A short-term shift of downy alder around 1.5 cal. ka BP, retreat of stone birch forest and advance of alder thickets between 1.7 and 1.27 cal. ka BP along with development of shrubby bogs with sweet gale and clubmoss around the lake confirm a span of milder and wetter conditions (Dirksen *et al.* 2015). Stone birch (*B. ermanii*) is a common tree in the interior mountain forests and prefers a mild climate and well-drained, even poor, nutrient substrates (Shamshin

1999) while the downy alder is a microthermic hygrophilous plant that needs very wet and mild conditions and prefers fertile substrates with a shallow groundwater table (Neshataeva & Kukurichkin 2003).

Another reconstructed cooling and possible short lake shallowing between 1.2–1.1 cal. ka BP fit in the second Late Holocene glacier advance in southeastern Kamchatka (Savoskul 1999). After 1.1 cal. ka BP cold stenotherm *P. austriacus*-type disappears from the record. The reconstructed T July rose to modern level and remained high until *c.* 0.9 cal. ka BP. A similar brief rise in chironomid-inferred summer temperatures around 1.0 cal. ka BP at Pechora Lake in the north of Kamchatka (Andrén *et al.* 2015) and at Two-Yurts Lake in central Kamchatka (Nazarova *et al.* 2013a) may be related to the MWP.

After 0.9 cal. ka BP, reconstructed T July remained below modern level until present. Indication of low temperatures arises as well from the increasing trend in the absolute number of chrysophyte cysts (Smol 1985; Rioual *et al.* 2007), although they do not necessarily indicate colder conditions and may depend on different ecological parameters (Lotter *et al.* 1997; Rioual *et al.* 2007). The last 1.2 ka, except for the uppermost spectrum, were characterized by minimal temperatures according to the record of forest distribution (Dirksen *et al.* 2015). As suggested by chironomids, diatom assemblages and vegetation composition, a cool climate, during the youngest interval of our record, is consistent with extended sea-ice coverage in the Okhotsk Sea (Koizumi *et al.* 2003), a temperature drop in central Kamchatka (Nazarova *et al.* 2013a; Hammarlund *et al.* 2015; Hoff *et al.* 2015; Meyer *et al.* 2015) and multiple Late Holocene glacier advances in central and southeastern Kamchatka after 1.0 cal. ka BP (Savoskul & Zech 1997; Savoskul 1999). Long-term cooling culminated during the Little Ice Age (LIA) around 0.15 cal. ka BP, as shown by tree-ring and ice-core records in Kamchatka (Solomina *et al.* 2007).

The chironomid and diatom communities of LS did not respond to the LIA or the following modern warming. However, the last 200 years are characterized by an occurrence of short-chained $n\mathrm{C}_{17}$ and $n\mathrm{C}_{19}$ alkanes (Fig. 3), often indicative of cyanobacteria and algal blooms (Bauersachs *et al.* 2017). This indicates a more productive lake. In the pollen record of LS, a prominent re-advance of stone birch forest most probably reflects the recent warming trend.

Many biological records suggest a prominent impact of the LIA on cooling across Kamchatka (Dirksen *et al.* 2013; Nazarova *et al.* 2013a; Andrén *et al.* 2015; Hoff *et al.* 2015; Solovieva *et al.* 2015; Nazarova *et al.* 2017a). It is also apparent in tree-ring and glacial records (Savoskul 1999; Solomina *et al.* 2007). Nonetheless, low taxonomic diversity or poor taxonomic and temporal resolution, and other factors like volcanic ashfalls could obscure the climatic response and cause spatial heterogeneity of responses (Brooks *et al.* 2015).

Our results detected several major Holocene climatic events (Early Holocene warming, HTM, Neoglacial, MWP) in the mountain region in the south of Kamchatka. These events are also found in many other records across Kamchatka and are apparent in climate records from the North Atlantic region (Brooks *et al.* 2015). However, our study confirms the earlier findings of spatial differences within Kamchatka in timing and magnitude of some of the major Holocene climate fluctuations. Onset of Early Holocene warming in the interior of the south of Kamchatka took place at least 1000 years later than at the northeast Pacific margin of the peninsula (Max *et al.* 2012; Brooks *et al.* 2015). In our data we as well observed a later beginning of the HTM relative to more northern sites in Kamchatka, continental areas of Siberia (Biskaborn *et al.* 2012; Nazarova *et al.* 2013b) and Chukotka (north of Kamchatka; Anderson & Lozhkin 2015). Our results support climate model experiments that suggest that the HTM was delayed in southern and central Kamchatka by about 2000 years compared with Alaska and NE Siberia (Jansen *et al.* 2007; Renssen *et al.* 2009, 2012). This gradual onset of the HTM has been explained by influence of post-glacial ice-sheet decay that modulated the westerly storm tracks in Eurasia (Renssen *et al.* 2009). Neoglacial cooling in Kamchatka is consistent with the strengthening of both the Siberian High and the Aleutian Low (Mayewski *et al.* 1997; Anderson *et al.* 2005; Jones *et al.* 2014; Hammarlund *et al.* 2015). Possible causes of the Medieval Warm Period include increased higher solar activity and lower volcanic activity (Schurer *et al.* 2014). The LIA cooling is related to another strengthening of the Siberian High and the Aleutian Low (Brooks *et al.* 2015), and the modern warming, though weakly traced in our record, is consistent with the modern observations (http://www.pogodaiklimat.ru/history/32540.htm).

Conclusions

In summary, chironomid and biomarker records from LS, a proglacial lake in south Kamchatka, reveal variable climatic conditions in the region during the Holocene. Fluctuations of limnic conditions are enhanced by the proximity of glacier that reacts sensitively to climatic changes. Consequently, chironomids and other proxy-indicators at the study site are responding not only to temperature, but also to changing lake depth that reflects changing runoff from the catchment. Although numerical reconstructions of the T July have moderate statistical significance, they are supported by biomarker, diatom and vegetation data, as well as available historical records across

Kamchatka. We have found that several climatic events influenced the lake and regional environmental history. Postglacial warming probably had an impact at higher elevations in central Kamchatka, initially between 10.0 and 9.0 cal. ka BP, which is about 1000 years later than on the Pacific coasts of Kamchatka. LS was formed after 10.0 cal. ka BP and was fed by glacial meltwaters from neighbouring glaciers in response to climate amelioration. Around 8.2 cal. ka BP the conditions in the interior peninsula became drier and cooler. This might be related to the 8.2 ka cooling event. The interval between 6.5 and 3.4 cal. ka BP can be attributed to the HTM with the warmest phase between 6.0 and 5.0 cal. ka BP, which is *c.* 2.0 ka later than in more northern sites of continental Siberia. The shift from an initially wet, maritime climate towards drier, more continental conditions after 6.0 cal. ka BP led to increasingly nutrient-enriched lake conditions, apparent in many lakes across Kamchatka. A clear change in dominants from less cold-tolerant *C. ambigua* to cold-stenotherm *C. oliveri*-type after 3.4 cal. ka BP followed the climatic deterioration and onset of Neoglacial cooling with the reconstructed T July ~1 °C below modern level. An abrupt short-term climatic cooling and strong lake shallowing between 1.8 and 1.5 cal. ka BP fits with a second glacial advance during the Late Holocene that occurred around 1.4–1.8 cal. ka BP. A short-term warming reconstructed between 1.2 and 0.9 cal. ka BP may be related to the MWP. Biological records of LS show only a weak response to the LIA or the following modern warming period.

Our results confirm the presence of teleconnections between the North Atlantic and North Pacific, modulating these climatic oscillations on a global scale. However, the revealed spatial differences in timing and magnitude of Holocene climatic events across Kamchatka demonstrate that more multi-proxy qualitative and especially quantitative palaeoecological studies are needed to better document the regional pattern in palaeoclimatic events and to unveil the background mechanisms driving the successions in ecosystems in the Kuril-Kamchatka region.

Acknowledgements. – We greatly appreciate the valuable scientific input of our highly respected colleague Dr Ulrike Hoff, who recently passed away, in the investigation of diatoms from Lake Sokoch, and studies of Kamchatka palaeoenvironments and taxonomy of diatoms. We thank all Russian colleagues who helped us during the fieldwork. This study was supported by Deutsche Forschungsgemeinschaft (DFG) Project NA 760/5-1 and DI 655/9-1. Our sincere thanks to the anonymous reviewers for their valuable comments. All data will be lodged with PANGEA upon publication.

Author contributions. – LN wrote the manuscript. VD, OD and BD executed the fieldwork for this project. LN and LS carried out the chironomid laboratory analysis. LN carried out statistical analysis of all data. DS and OR carried out the biomarker analysis. HF contributed to the landscape analyses. BD and NR contributed to the overall interpretation of the data. VD and OD provided regional information. All authors contributed to manuscript production.

References

Alley, R. B., Mayewski, P. A., Sowers, T., Stuiver, M., Taylor, K. C. & Clark, P. U. 1997: Holocene climatic instability: a prominent, widespread event 8200 years ago. *Geology 25*, 483–486.

Anderson, L., Abbott, M. B., Finney, B. P. & Burns, S. J. 2005: Regional atmospheric circulation in the North Pacific during the Holocene inferred from lacustrine carbonate oxygen isotopes, Yukon Territory, Canada. *Quaternary Research 64*, 21–35.

Anderson, P. M. & Lozhkin, A. V. 2015: Late Quaternary vegetation of Chukotka (Northeast Russia), implications for Glacial and Holocene environments of Beringia. *Quaternary Science Reviews 107*, 112–128.

Andrén, E., Klimaschewski, A., Self, A. E., St. Amour, N., Andreev, A. A., Bennett, K. D., Conley, D. J., Edwards, T. W. D., Solovieva, N. & Hammarlund, D. 2015: Holocene climate and environmental change in north-eastern Kamchatka (Russian Far East). *Global and Planetary Change 134*, 41–54.

Barley, E. M., Walker, I. R., Kurek, J., Cwynar, L. C., Mathewes, R. W., Gajewski, K. & Finney, B. P. 2006: A northwest North American training set: distribution of freshwater midges in relation to air temperature and lake depth. *Journal of Paleolimnology 36*, 295–314.

Barr, I. D. & Solomina, O. 2014: Pleistocene and Holocene glacier fluctuations upon the Kamchatka Peninsula. *Global and Planetary Change 113*, 110–120.

Bauersachs, T., Talbot, H. M., Sidgwick, F., Sivonen, K. & Schwark, L. 2017: Lipid biomarker signatures as tracers for harmful cyanobacterial blooms in the Baltic Sea. *PLoS ONE 12*, e0186360, https://doi.org/10.1371/journal.pone.0186360.

Berglund, B. E. & Digerfeldt, G. 1970: A palaeoecological study of the Late-Glacial lake at Torreberga, Scania, south Sweden. *Oikos 21*, 98–128.

Birks, H. J. B. 1995: Quantitative palaeoenvironmental reconstructions. *In* Maddy, D. & Brew, J. S. (eds.): *Statistical Modelling of Quaternary Science Data. Technical Guide 5*, 161–254. Quaternary Research Association, Cambridge.

Birks, H. J. B. & Gordon, A. D. 1985: *Numerical Methods in Quaternary Pollen Analysis.* 317 pp. Academic Press, London.

Birks, H. J. B., Line, J. M., Juggins, S., Stevenson, A. C. & ter Braak, C. J. F. 1990: Diatoms and pH reconstruction. *Philosophical Transactions of the Royal Society of London, Series B 327*, 263–278.

Biskaborn, B. K., Herzschuh, U., Bolshiyanov, D., Savelieva, L., Zibulski, R. & Diekmann, B. 2012: Late Holocene thermokarst variability inferred from diatoms in a lake sediment record from the Lena Delta, Siberian Arctic. *Journal of Paleolimnology 49*, 155–170.

Biskaborn, B. K., Nazarova, L., Pestryakova, L. A., Syrykh, L., Funck, K., Meyer, H., Chapligin, B., Vyse, S., Gorodnichev, R., Zakharov, E., Wang, R., Schwamborn, G. & Diekmann, B. 2019: Spatial distribution of environmental indicators in surface sediments of Lake Bolshoe Toko, Yakutia, Russia. *Biogeosciences 16*, 4023–4049.

ter Braak, C. J. F. 1995: Ordination. *In* Jongman, R. H. G., ter Braak, C. J. F. & van Tongeren, O. F. R. (eds.): *Data Analysis in Community and Landscape Ecology*, 69–173. Cambridge University Press, Cambridge.

ter Braak, C. J. F. & Prentice, I. C. 1988: A theory of gradient analysis. *Advances in Ecological Research 18*, 271–317.

ter Braak, C. J. F. & Šmilauer, P. 2002: *CANOCO Reference Manual and CanoDraw for Windows User's Guide: Software for Canonical Community Ordination Version 4.5*. Microcomputer Power, Ithaca, NY. www.canoco.com.

ter Braak, C. J. F., Juggins, S., Birks, H. J. B. & van der Voet, H. 1993: Weighted averaging partial least squares regression (WA-PLS): definition and comparison with other methods for species-environment calibration. *In* Patil, G. P. & Rao, C. R. (eds.): *Multivariate Environmental Statistics*, 525–560, Elsevier Science Publishers B.V, Amsterdam.

Braitseva, O. A., Melekeszev, I. V., Evteeva, I. S. & Lupikina, E. G. 1968: *Quaternary Stratigraphic Deposits and Glaciations of Kamchatka*. 227 pp. Nauka, Moscow (in Russian).

Braitseva, O. A., Ponomareva, V. V., Sulerzhitsky, L. D., Melekestsev, I. V. & Bailey, J. 1997: Holocene key-marker tephra layers in Kamchatka, Russia. *Quaternary Research 47*, 125–139.

Brodersen, K. P. & Lindegaard, C. 1999: Mass occurrence and sporadic distribution of *Corynocera ambigua* Zettersted (Diptera, Chironomidae) in Danish lakes. Neo- and paleolimnological records. *Journal of Paleolimnology 22*, 41–52.

Brodin, Y. 1986: The postglacial history of Lake Flarken, southern Sweden, interpreted from subfossil insect remains. *Internationale Revue der gesamten Hydrobiologie 71*, 371–432.

Brooks, S. J., Diekmann, B., Jones, V. J. & Hammarlund, D. 2015: Holocene environmental change in Kamchatka: a synopsis. *Global and Planetary Change 134*, 166–174.

Brooks, S. J., Langdon, P. G. & Heiri, O. 2007: *The Identification and Use of Palaearctic Chironomidae Larvae in Palaeoecology.* 276 pp. Quaternary Research Association, London.

Chao, A., Gotelli, N. J., Hsieh, T. C., Sande, E. L., Ma, K. H., Colwell, R. K. & Ellison, A. M. 2014: Rarefaction and extrapolation with Hill numbers: a framework for sampling and estimation in species diversity studies. *Ecological Monographs 84*, 45–67.

Cremer, H., Bunnik, F. P. M. & Lammens, E. H. R. R. 2007: Diatom paleoecology of Lake Ijssel, The Netherlands. *Diatomededelingen 31*, 39–43.

Danzeglocke, U., Jöris, O. & Weninger, B. 2010: *CalPal-2007online.* Available at: http://www.calpal-online.de/.

Dirksen, V., Dirksen, O., van den Bogaard, C. & Diekmann, B. 2015: Holocene pollen record from Lake Sokoch, interior Kamchatka (Russia), and its palaeobotanical and paleoclimatic interpretation. *Global and Planetary Change 134*, 129–141.

Dirksen, V., Dirksen, O. & Diekmann, B. 2013: Holocene vegetation dynamics and climate change in Kamchatka Peninsula, Russian Far East. *Review of Palaeobotany and Palynology 190*, 48–65.

Engels, S., Cwynar, L. C., Shuman, B. N. & Rees, A. B. H. 2012: Chironomid-based water depth reconstructions: an independent evaluation of site-specific and local inference models. *Journal of Paleolimnology 48*, 693–709.

Engels, S., Medeiros, A. S., Axford, Y., Brooks, S. J., Heiri, O., Luoto, T. P., Nazarova, L., Porinchu, D. F., Quinlan, R. & Self, A. E. 2020: Temperature change as a driver of spatial patterns and long-term trends in chironomid (Insecta: Diptera) diversity. *Global Change Biology 26*, 1155–1169.

Feakins, S. J. & Sessions, A. L. 2010: Controls on the D/H ratios of plant leaf waxes in an arid ecosystem. *Geochimica et Cosmochimica Acta 74*, 2128–2141.

Ficken, K., Li, B., Swain, D. & Eglinton, G. 2000: An n-alkane proxy for the sedimentary input of submerged/floating freshwater aquatic macrophytes. *Organic Geochemistry 31*, 745–749.

Fjellberg, A. 1972: Present and Late Weichselian occurrence of *Corynocera ambigua* Zett. (Dipt., Chironomidae) in Norway. *Norsk Entomologisk Tidsskrift 19*, 59–61.

Frolova, L. A., Nazarova, L., Pestryakova, L. & Herzschuh, U. 2013: Analysis of the effects of climate-dependent factors on the formation of zooplankton communities that inhabit arctic lakes in the Anabar river basin. *Contemporary Problems of Ecology 6*, 1–11.

Gat, J. R. 1996: Oxygen and hydrogen isotopes in the hydrologic cycle. *Annual Review of Earth and Planetary Sciences 24*, 225–262.

Gledhill, D. 2007: *Kamchatka: A Journey and Guide to Russia's Land of Ice and Fire.* 311 pp. Odyssey Books and Guides, Hong Kong.

Guy-Ohlson, D. 1992: Botryococcus as an aid in the interpretation of palaeoenvironment and depositional processes. *Review of Palaeobotany and Palynology 71*, 1–15.

Halkiewicz, A. 2009: *Corynocera ambigua* (Insecta, Diptera) subfossils occurrence in recent sediments of four shallow Polesie lakes. *Annals universitatis Mariae Curie-Skłodowska Lublin – Polonia 2*, 31–36.

Hammarlund, D., Klimaschewski, A., Amour, N. A. S., Andrén, E., Self, A. E., Solovieva, N., Andreev, A. A., Barnekow, L. & Edwards, T. W. D. 2015: Late Holocene expansion of Siberian dwarf pine (*Pinus pumila*) in Kamchatka in response to increased snow cover as inferred from lacustrine oxygen isotope records. *Global and Planetary Change 134*, 91–100.

Hammarlund, D., Klimaschewski, A., St. Amour, N. A., Andreev, A. A., Andrén, A., Barnekow, L. & Edwards, T. W. D. 2012: Late Holocene increase in winter snow-cover in Kamchatka followed by wide-spread expansion of Siberian dwarf pine (*Pinus pumila*). 2nd BIOCOLD workshop, Kernaves, Lithuania, April 25–27.

Heiri, O. & Lotter, A. F. 2001: Effect of low count sums on quantitative environmental reconstructions: an example using subfossil chironomids. *Journal of Paleolimnology 26*, 343–350.

Heiri, O., Brooks, S. J., Renssen, H., Bedford, A., Hazekamp, M., Ilyashuk, B., Jeffers, E. S., Lang, B., Kirilova, E., Kuiper, S., Millet, L., Samartin, S., Toth, M., Verbruggen, F., Watson, J. E., van Asch, N., Lammertsma, E., Amon, L., Birks, H. H., Birks, H. J. B., Mortenson, M. F., Hoek, W. Z., Magyari, E., Muñoz Sobrino, C., Seppä, H., Tinner, W., Tonkov, S., Veski, S. & Lotter, A. F. 2014: Validation of climate model-inferred regional temperature change for late-glacial Europe. *Nature Communications 5*, 4914, https://doi.org/10.1038/ncomms5914.

Hill, M. O. 1973: Diversity and evenness: a unifying notation and its consequences. *Ecology 54*, 427–432.

Hoff, U., Biskaborn, B. K., Dirksen, V., Dirksen, O., Kuhn, G., Meyer, H., Nazarova, L., Roth, A. & Diekmann, B. 2015: Holocene environment of Central Kamchatka, Russia: implications from a multi-proxy record of Two-Yurts Lake. *Global and Planetary Change 134*, 101–117.

Hoff, U., Dirksen, O., Dirksen, V., Kuhn, G., Meyer, H. & Diekmann, B. 2014: Holocene freshwater diatoms: palaeoenvironmental implications from south Kamchatka, Russia. *Boreas 43*, 22–41.

Hofmann, W. 1978: Analysis of animal microfossils from the Groper Segeberger See. *Archiv für Hydrobiologie 82*, 316–346.

Hofmann, W. 1983a: Stratigraphy of subfossil Chironomidae and Ceratopogonidae (Insecta: Diptera) in late glacial littoral sediments from Lobsigensee (Swiss Plateau). Studies in the late Quaternary of Lobsigensee 4. *Revue de Paleobiologie 2*, 205–209.

Hofmann, W. 1983b: Stratigraphy of Cladocera and Chironomidae in a core from a shallow North German Lake. *Hydrobiologia 103*, 235–239.

Hsieh, T. C., Ma, K. H. & Chao, A. 2020: *iNEXT: Interpolation and Extrapolation for Species Diversity. R package version 2.0.20*, http://chao.stat.nthu.edu.tw/wordpress.

Itaki, T. & Ikehara, K. 2004: Middle to late Holocene changes of the Okhotsk Sea Intermediate Water and their relation to atmospheric circulation. *Geophysical Research Letters 31*, L24309. https://doi.org/10.1029/2004GL021384.

Jansen, E., Overpeck, J., Briffa, K. R., Duplessy, J.-C., Joos, F., Masson-Delmotte, V., Olago, D., Otto-Bliesner, B., Peltier, W. R., Rahmstorf, S., Ramesh, R., Raynaud, D., Rind, D., Solomina, O., Villalba, R. & Zhang, D. 2007: Palaeoclimate. *In* Solomon, S., Qin, D., Manning, M., Chen, Z., Marquis, M., Averyt, K. B., Tignor, M. & Miller, H. L. (eds.): *Climate Change 2007: The Bhysical Science basis; Contribution of Working Group I to the Fourth Assessment Report of the Intergovernmental Panel on Climate Change*, 433–497. Cambridge University Press, Cambridge.

Jones, V. & Solomina, O. 2015: The geography of Kamchatka. *Global and Planetary Change 134*, 3–9.

Jones, M. C., Wooller, M., Peteet, D. M. & Katsuki, K. 2014: A deglacial and Holocene record of climate variability in south-central Alaska from stable oxygen isotopes and plant macrofossils in peat. *Quaternary Science Reviews 87*, 1–11.

Juggins, S. 2001: *The European Diatom Database. User Guide Version 1.0*. 72 pp. University of Newcastle, Newcastle upon Tyne.

Juggins, S. 2007: *C2 Version 1.5 User Guide. Software for Ecological and Palaeoecological Data Analysis and Visualization*. 73 pp. Newcastle University, Newcastle upon Tyne.

Juggins, S. & Birks, H. J. B. 2012: Quantitative environmental reconstructions from biological data. *In* Birks, H. J. B., Lotter, A. F., Juggins, S. & Smol, J. P. (eds.): *Tracking Environmental Change Using Lake Sediments. Data Handling and Numerical Techniques*, 431–494. Springer, Dordrecht.

Kahmen, A., Hoffmann, B., Schefuß, E., Arndt, S. K., Cernusak, L. A., West, J. B. & Sachse, D. 2013: Leaf water deuterium enrichment shapes leaf wax n-alkane δD values of angiosperm plants II: Observational evidence and global implications. *Geochimica et Cosmochimica Acta 111*, 50–63.

Kaufman, D. S., Schneider, D. P., McKay, N. P., Ammann, C. M., Bradley, R. S., Briffa, K. R., Miller, G. H., Otto-Bliesner, B. L., Overpeck, J. T. & Vinther, B. M. 2009: Recent warming reverses long-term Arctic cooling. *Science 325*, 1236–1239.

Kerschner, H., Hertl, A., Gross, G., Ivy-Ochs, S. & Kubik, P. W. 2006: Surface exposure dating of moraines in the Kromer valley (Silvretta Mountains, Austria) - evidence for glacial response to the 8.2 ka event in the Eastern Alps. *The Holocene 16*, 7–15.

Klimaschewski, A., Barnekow, L., Bennett, K. D., Andreev, A. A., Andrén, E., Bobrov, A. A. & Hammarlund, D. 2015: Holocene environmental changes in southern Kamchatka, Eastern Russia, inferred from a pollen and testate amoebae record from a peat succession. *Global and Planetary Change 134*, 142–154.

Koizumi, I., Shiga, K., Irino, T. & Ikehara, M. 2003: Diatom record of the late Holocene in the Okhotsk Sea. *Marine Micropaleontology 49*, 139–156.

Larocque, I. 2001: How many chironomid head capsules is enough? A statistical approach to determine sample size for paleoclimatic reconstruction. *Palaeogeography, Palaeoclimatology, Palaeoecology 172*, 133–142.

Lotter, A. F. & Biegler, C. 2000: Do diatoms in the Swiss Alps reflect the length of ice-cover? *Aquatic Sciences 62*, 125–141.

Lotter, A. F. & Juggins, S. 1991: POLPROF, TRAN and ZONE: programs for plotting, editing and zoning pollen and diatom data. *INQUA-Subcommission for the Study of the Holocene Working Group on Data-Handling Methods, Newsletter 6*, 4–6.

Lotter, A. F., Birks, H. J. B., Hofmann, W. & Marchetto, A. 1997: Modern diatom, cladocera, chironomid, and chrysophyte cyst assemblages as quantitative indicators for the reconstruction of past environmental conditions in the Alps. I. Climate. *Journal of Paleolimnology 18*, 395–420.

Lozhkin, A. V., Anderson, P., Eisner, W. R. & Solomatkina, T. B. 2011: Late glacial and Holocene landscapes of central Beringia. *Quaternary Research 76*, 383–392.

Max, L., Riethdorf, R. R., Tiedemann, R., Smirnova, M., Lembke-Jene, L., Fahl, K., Nürnberg, D., Matul, A. & Mollenhauer, G. 2012: Sea surface temperature variability and sea-ice extent in the subarctic northwest Pacific during the past 15,000 years. *Paleoceanography 27*, PA3213, https://doi.org/10.1029/2012PA002292.

Mayewski, P. A., Meeker, L. D., Twickler, M. S., Whitlow, S., Yang, Q., Lyons, W. B. & Prentice, M. 1997: Major features and forcing of high-latitude northern hemisphere atmospheric circulation using a 110,000-year-long glaciochemical series. *Journal of Geophysical Research 102*, 26345–26366.

Mayewski, P. A., Rohling, E. E., Stager, J. C., Karlén, K. A., Maasch, W., Meeker, L. D., Meyerson, E. A., Gasse, F., van Kreveld, S., Holmgren, K., Lee-Thorp, J., Rosqvist, G., Rack, F., Staubwasser, M., Schneider, R. R. & Steiger, E. J. 2004: Holocene climate variability. *Quaternary Research 62*, 243–255.

Meyer, H., Chapligin, B., Hoff, U., Nazarova, L. & Diekmann, B. 2015: Oxygen isotope composition of diatoms as Late Holocene climate proxy at Two-Yurts-Lake, Central Kamchatka, Russia. *Global and Planetary Change 134*, 118–128.

Meyers, P. A. & Teranes, J. L. 2001: Sediment organic matter. *In* Last, W. M. & Smol, J. P. (eds.): *Tracking Environmental Change Using Lake Sediments. Physical and Geochemical Methods*, 239–269. Kluwer, Dordrecht.

Moller Pillot, H. K. M. 2009: *Chironomidae Larvae. Biology and Ecology of the Chironomini*. 270 pp. KNNV Publishing, Zeist.

Moller Pillot, H. K. M. 2013: *Chironomidae Larvae of the Netherlands and Adjacent Lowlands. Biology and Ecology of the Aquatic Orthocladiinae*. 312 pp. KNNV Publishing, Zeist.

Nazarova, L., Bleibtreu, A., Hoff, U., Dirksen, V. & Diekmann, B. 2017a: Changes in temperature and water depth of a small mountain lake during the past 3000 years in Central Kamchatka reflected by chironomid record. *Quaternary International 447*, 46–58.

Nazarova, L., Grebennikova, T. A., Razjigaeva, N. G., Ganzey, L. A., Belyanina, N. I., Arslanov, K. A., Kaistrenko, V. M., Gorbunov, A. O., Kharlamov, A. A., Rudaya, N., Palagushkina, O., Biskaborn, B. K. & Diekmann, B. 2017b: Reconstruction of Holocene environmental changes in Southern Kurils (North-Western Pacific) based on palaeolake sediment proxies from Shikotan Island. *Global and Planetary Change 159*, 25–36.

Nazarova, L., Herzschuh, U., Wetterich, S., Kumke, T. & Pestjakova, L. 2011: Chironomid-based inference models for estimating mean July air temperature and water depth from lakes in Yakutia, northeastern Russia. *Journal of Paleolimnology 45*, 57–71.

Nazarova, L., de Hoog, V., Hoff, U., Dirksen, O. & Diekmann, B. 2013a: Late Holocene climate and environmental changes in Kamchatka inferred from the subfossil chironomid record. *Quaternary Science Reviews 67*, 81–92.

Nazarova, L., Lüpfert, H., Subetto, D., Pestryakova, L. & Diekmann, B. 2013b: Holocene climate conditions in Central Yakutia (North-Eastern Siberia) inferred from sediment composition and fossil chironomids of Lake Temje. *Quaternary International 290–291*, 264–274.

Nazarova, L., Pestryakova, L. A., Ushnitskaya, L. & Hubberten, H.-W. 2008: Chironomids (Diptera: Chironomidae) in lakes of central Yakutia and their indicative potential for paleoclimatic research. *Contemporary Problems of Ecology 1*, 335–345.

Nazarova, L., Razjigaeva, N. G., Golovatuk, L. G., Biskaborn, B. K., Grebennikova, T. A., Ganzey, L. A., Mokhova, L. M. & Diekmann, B. 2021a: Development of ecological conditions in East Prymorje in Holocene. *Contemporary Problems of Ecology 14*, 218–230.

Nazarova, L., Razjigaeva, N. G., Ganzey, L. A., Makarova, T. R., Lyaschevskaya, M. S., Biskaborn, B. K., Hoelzmann, P. & Diekman, B. 2021b: Mid- to Late Holocene environment of the Iturup Island (Kurils, North Western Pacific). *Quaternary International in press*, https://doi.org/10.1016/j.quaint.2021.05.003.

Nazarova, L., Self, A. E., Brooks, S. J., van Hardenbroek, M., Herzschuh, U. & Diekmann, B. 2015: Northern Russian chironomid-based modern summer temperature data set and inference models. *Global and Planetary Change 134*, 10–25.

Nazarova, L., Self, A. E., Brooks, S. J., Solovieva, N., Syrykh, L. S. & Dauvalter, V. A. 2017c: Chironomid fauna of the lakes from the Pechora River basin (East of European part of Russian Arctic): ecology and reconstruction of recent ecological changes in the region. *Contemporary Problems of Ecology 4*, 350–362.

Nazarova, L., Syrykh, L. S., Mayfield, R. J., Frolova, L. A., Ibragimova, A. G., Grekov, I. M. & Subetto, D. A. 2020: Palaeoecological and palaeoclimatic conditions in Karelian Isthmus (northwestern Russia) during the Holocene: multi-proxy analysis of sediments from the Lake Medvedevskoe. *Quaternary Research 95*, 65–83.

Neshataeva, V. Yu. & Kukurichkin, G. M. 2003: Rare plant communities of *Alnus hirsuta* (Betulaceae) in the Kikhchik River basin (western Kamchatka). *Botanicheskii Zhurnal 88*, 90–99 (in Russian with English summary).

Oliver, D. R. & Roussel, M. E. 1983: The insects and arachnids of Canada. Part 11. The genera of larval midges of Canada; Diptera: Chironomidae. *Agriculture Canada, Research Branch 1746*, 1–263.

Palagushkina, O. V., Nazarova, L., Wetterich, S. & Shirrmaister, L. 2012: Diatoms of modern bottom sediments in Siberian Arctic. *Contemporary Problems of Ecology 5*, 413–422.

Palagushkina, O., Wetterich, S., Biskaborn, B., Nazarova, L., Lenz, J., Schwamborn, G., Schirrmeister, L. & Grosse, G. 2017: Diatom records and tephra mineralogy in pingo deposits of Seward Peninsula, Alaska. *Palaeogeography, Palaeoclimatology, Palaeoecology 479*, 1–15.

Pinder, L. C. V. & Reiss, F. 1983: The larvae of Chironominae (Diptera: Chironomidae) of Holarctic region – keys and diagnoses. *In* Wiederholm T. (ed.): *Chironomidae of the Holarctic Region. Keys and Diagnoses. Part 1 – Larvae*, 293–435. *Entomologica Scandinavica, Supplement 19*. Motala, Lund.

Plikk, A., Engels, S., Luoto, T., Nazarova, L., Salonen, J. S. & Helmens, K. F. 2019: Chironomid-based temperature reconstruction for the Eemian Interglacial (MIS 5e) at Sokli, northeast Finland. *Journal of Paleolimnology 61*, 355–371.

Ponomareva, V. V., Kyle, P. R., Pevzner, M., Sulerzhitsky, L. D. & Hartman, M. 2007: Holocene eruptive history of Shiveluch volcano, Kamchatka Peninsula. *In* Eichelberger, J., Ordeev, E., Asahara, M., Izbekov, P. & Lees, J. (eds.): *Volcanism and Subduction: The Kamchatka Region*, 263–282. *American Geophysical Union Geophysical Monograph Series 172*.

Porinchu, D. F. & Cwynar, L. C. 2000: The distribution of freshwater Chironomidae (Insecta: Diptera) across the treeline near the lower

Lena River, northeast Siberia. *Arctic, Antarctic, and Alpine Research 32*, 429–437.

Quinlan, R. & Smol, J. P. 2001: Setting minimum head capsule abundance and taxa deletion criteria in chironomid-based inference models. *Journal of Paleolimnology 26*, 327–342.

R Core Team 2012: *R: Language and Environment for Statistical Computing*. R Foundation for Statistical Computing, Vienna, Austria.

Reiss, F. & Gerstmeier, R. 1984: *Corynocera ambigua* Zetterstedt als Glazialrelikt im Starnberger See, Oberbayern. *Nachrichtenblatt der Bayersichen Entomologie 33*, 58–61.

Renssen, H., Seppä, H., Crosta, X., Goosse, H. & Roche, D. M. 2012: Global characterization of the Holocene Thermal Maximum. *Quaternary Science Reviews 48*, 7–19.

Renssen, H., Seppä, H., Heiri, O., Roche, D. M., Goosse, H. & Fichefet, T. 2009: The spatial and temporal complexity of the Holocene thermal maximum. *Nature Geoscience 2*, 411–414.

Riera, S., López-Sáez, J. A. & Juliá, R. 2006: Lake responses to historical land use changes in northern Spain: the contribution of non-pollen palynomorphs in a multiproxy study. *Review of Palaeobotany and Palynology 141*, 127–138.

Rioual, P., Andrieu-Ponel, V., de Beaulieu, J. L., Reille, M., Svobodova, H. & Battarbee, R. W. 2007: Diatom responses to limnological and climatic changes at Ribains Maar (French Massif Central) during the Eemian and Early Würm. *Quaternary Science Reviews 26*, 1557–1609.

Sachse, D., Billault, I., Bowen, G. J., Chikaraishi, Y., Dawson, T. E., Feakins, S. J., Freeman, K. H., Magill, C. R., McInerney, F. A., van der Meer, M. T. J., Polissar, P., Robins, R. J., Sachs, J. P., Schmidt, H.-L., Sessions, A. L., White, J. W. C., West, J. B. & Kahmen, A. 2012: Molecular paleohydrology: interpreting the hydrogen-isotopic composition of lipid biomarkers from photosynthesizing organisms. *Annual Review of Earth and Planetary Sciences 40*, 221–249.

Sachse, D., Gleixner, G., Wilkes, H. & Kahmen, A. 2010: Leaf wax n-alkane delta D values of field-grown barley reflect leaf water delta D values at the time of leaf formation. *Geochimica et Cosmochimica Acta 74*, 6741–6750.

Savoskul, O. S. 1999: Holocene glacier advances in the headwaters of Sredniaya Avacha, Kamchatka, Russia. *Quaternary Research 52*, 14–26.

Savoskul, O. S. & Zech, W. 1997: Holocene glacier advances in the Topolovaya Valley, Bystrinskiy Gange, Kamchatka, Russia, dated by tephrochronology and lichenometry. *Arctic, Antarctic, and Alpine Research 29*, 143–155.

Schakau, B. & Frank, C. 1984: Die Entwicklung der Chironomiden-Fauna (Diptera) des Tegeler Sees im Spat- und Postglazial. *Verhandlungen der Gesellschaft für Ökologie 12*, 375–382.

Schurer, A. P., Tett, S. F. B. & Hegerl, G. C. 2014: Small influence of solar variability on climate over the past millennium. *Nature Geoscience 7*, 104–108.

Self, A. E., Klimaschewski, A., Solovieva, N., Jones, V. J., Andrén, E., Andreev, A. A., Hammarlund, D. & Brooks, S. J. 2015: Holocene environmental changes inferred from a mountain lake in central Kamchatka. *Global and Planetary Change 134*, 67–81.

Shamshin, V. A. 1999: *Stone Birch Forest of Kamchatka*. 169 pp. Geos, Moscow (in Russian).

Smol, J. P. 1985: The ratio of diatom frustules to chrysophycean statospores: a useful paleolimnological index. *Hydrobiologia 123*, 199–208.

Solomina, O., Wiles, G., Shiraiwa, T. & D'Arrigo, R. 2007: Multiproxy records of climate variability for Kamchatka for the past 400 years. *Climate of the Past 3*, 119–128.

Solovieva, N., Klimaschewski, A., Self, A. E., Jones, V. J., Andrén, E., Andreev, A. A., Hammarlund, D., Lepskaya, E. V. & Nazarova, L. 2015: Holocene environmental history of a small coastal lake from north-eastern Kamchatka Peninsula. *Global and Planetary Change 134*, 55–66.

Stief, P., Nazarova, L. & De Beer, D. 2005: Chimney construction by *Chironomus riparius* larvae in response to hypoxia: microbial implications for freshwater sediments. *Journal of the North American Benthological Society 24*, 858–871.

Subetto, D. A., Nazarova, L., Pestryakova, L. A., Syrykh, L. S., Andronikov, A. V., Biskaborn, B. K., Diekmann, B., Kuznetsov, D. D., Sapelko, T. V. & Grekov, I. M. 2017: Palaeolimnological studies in Russian Northern Eurasia: a review. *Contemporary Problems of Ecology 4*, 327–335.

Syrykh, L. S., Nazarova, L., Herzschuh, U., Subetto, D. A. & Grekov, I. M. 2017: Reconstruction of palaeoecological and palaeoclimatic conditions of the Holocene in the south of Taimyr according to the analysis of lake sediments. *Contemporary Problems of Ecology 4*, 363–369.

Tierney, J. E., Russell, J. M., Huang, Y., Damste, J. S. S., Hopmans, E. C. & Cohen, A. S. 2008: Northern hemisphere controls on tropical southeast African climate during the past 60,000 years. *Science 322*, 252–255.

Walker, I. R. & Mathewes, R. W. 1988: Late Quaternary fossil Chironomidae (Diptera) from Hippa Lake, Queen Charlotte Islands, British Columbia, with special reference to *Corynocera* Zett. *Canadian Entomologist 120*, 739–751.

Wetterich, S., Schirrmeister, L., Nazarova, L., Palagushkina, O., Bobrov, A., Pogosyan, L., Savelieva, L., Syrykh, L., Matthes, H., Fritz, M., Gunther, F. & Opel, T. 2018: Holocene thermokarst and pingo development in the Kolyma Lowland 1 (NE Siberia). *Permafrost and Periglacial Processes 29*, 182–198.

Wetzel, R. G. 2001: *Limnology: Lake and River Ecosystems.* 1006 pp. Academic Press, San Diego.

Wiederholm, T. 1983: *Chironomidae of the Holarctic region. Keys and diagnoses. Part 1. Larvae.* 457 pp. *Entomologica Scandinavica, Supplement 19*. Borgströms Tryckeri AB, Motala, Lund.

Yamagata, K., Sone, T., Sawagaki, T. & Muravyev, Y. D. 2002: Holocene fluctuations of the Bilchenok Glacier, Kamchatka Peninsula. *Journal of Geography 111*, 509–518.

Yamagata, K., Sone, T., Sawagaki, T., Otsuki, Y. & Muravyev, Y. D. 2000: Holocene glacial history of the Kamchatka Peninsula. *In* Wakatsuchi, M. & Hara, T. (eds.): *Proceedings of International Symposium on Atmosphere–Ocean–Cryosphere Interaction in the Sea of Okhotsk and the Surrounding Environment*, 164–165. Institute of Low Temperature, Hokkaido University, Sapporo.

Supporting Information

Additional Supporting Information may be found in the online version of this article at http://www.boreas.dk.

Table S1. Radiocarbon dates on the sediments from Lake Sokoch (following Hoff *et al.* 2014).

Fig. S1. Chironomid-inferred T July; PCA axes 1 and 2 scores for chironomid data; results of goodness-of-fit (GoF) tests for reconstructed T July, with 90th and 95th percentiles of the residual distances of all the modern samples that are identified as samples with a 'poor fit' and a 'very poor fit' with the reconstructed T July; sums of rare and absent taxa in the T July training sets (Nazarova *et al.* 2015).

Fig. S2. Down-core variation of $n\mathrm{C}_{17}$ and $n\mathrm{C}_{19}$ alkanes.

Fig. S3. Down-core variations of sediment core PG1890-1: PCA 1 of chironomid, diatom, pollen and biomarker data; sedimentological data. Thin blue bars represent horizons of volcanic ash layers with names of the tephras at the right side. Grey bar represents mudflow. For PCA 1 of the diatom data and T July, red lines represent LOESS 0.2 smoothing of the data. Dashed lines differentiate chironomid assemblage zones I to VI (CH I–VI).